TECHNISCHE UNIVERSITÄT WIEN
Vienna University of Technology

DISSERTATION

Effectors of DNA accessibility in *Trichoderma reesei*

ausgeführt zum Zwecke der Erlangung des akademischen Grades einer Doktorin der technischen Wissenschaften unter Leitung von

Prof. Dr. Robert Mach und
Priv. Doz. Dr. Astrid Mach-Aigner
E166
Institut für Verfahrenstechnik, Umwelttechnik und Technische Biowissenschaften

eingereicht an der Technischen Universität Wien,
Fakultät für Technische Chemie

von

DI Alice Rassinger, BSc
0625851
Wallgasse 30/9-10, 1060 Wien

Wien, am

Table of Content

Kurzfassung

Der filamentöse Pilz *Trichoderma reesei* ist von Natur aus fähig pflanzliche Biomasse abzubauen. Er sondert eine Reihe von hydrolytischen Enzymen in seine Umgebung ab, die das pflanzliche Material, das zum größten Teil aus Zellulose und Hemizellulose besteht, in niedermolekulare Kohlehydrate zerlegen. Die Abbauprodukte stehen nun dem Pilz zur Nahrungsaufnahme zur Verfügung. Je nachdem, welche Kohlehydrate in der Umgebung vorhanden sind, werden die regulatorischen Schaltkreise des Pilzes daran angepasst. Damit gibt es auch ein bevorzugtes Substrat für die Zellulasen- und Hemizellulasenproduktion. Beispielsweise übt der Einfachzucker D-Glukose, der leicht zu verstoffwechseln ist, eine Katabolitrepression auf die hydrolytischen Enzyme aus. Die Aufnahme solcher Einfachzucker wird priorisiert und die Energie wird vor allem in Biomassebildung und Selbsterhaltung gesteckt. Das stellt besonders für die industrielle Enzymproduktion eine große Herausforderung dar. Um dieses unerwünschte Phänomen zu umgehen, wurden Stämme wie Rut-C30 durch zufällige Mutagenese auf erhöhte Zellulaseproduktion erstellt. Die meisten Industriesstämme haben einen ähnlichen genetischen Hintergrund wie die Mutante Rut-C30. Zu diesen genetischen Merkmalen zählen die erhöhte Zellulaseproduktion und die fehlende Katabolitrepression auf D-Glukose. Es ist jedoch noch unklar, welches genetische Merkmal nun für den Rut-C30-Phänotyp konkret ausschlaggebend ist, da durch die zufällige Mutagenese eine Reihe von Mutationen aufgetreten sind.

Die Kontrolle der Expression der hydrolytischen Enzyme erfolgt zu einem großen Teil durch den Transaktivator Xyr1 und das Katabolit-Repressor-Protein Cre1. Beide Transkriptionsfaktoren agieren in einer Abhängigkeit von bestimmten Zuckern. Bisher ist viel über das Zusammenspiel von Cre1 und Xyr1 und deren Einfluss auf die Zellulase- und Xylanaseexpression bekannt. Es ist jedoch zu bedenken, dass der Pilz (wie jeder andere Eukaryot) seine DNA mittels Histonproteine verpackt und dadurch die lokale Genstruktur eine andere Zugänglichkeit für bestimmte Faktoren bekommt. Dies führt zu einem zusätzlichen Aspekt in der Genregulation, der berücksichtigt werden muss und auch gezielt genutzt werden kann.

Diese Dissertation untersucht die verschiedenen Einflüsse auf die DNA-Zugänglichkeit und die weiteren Folgerungen für die Zellulase- und Xylanaseexpression. Die DNA-Zugänglichkeit kann durch Änderungen in der Chromatinstruktur und durch das Bindeverhalten von bestimmten Transkriptionsfaktoren, wie zum Beispiel, Cre1 verändert werden. Zur Wirkungsweise der jeweiligen Einflüsse wurden Transkriptionsanalysen und Chromatinzugänglichkeiten bestimmt. Sowohl D-Xylose als auch α-Sophorose, induzieren in

Trichoderma die Expression der Xylanasen. In beiden Fällen trägt die Chromatinstruktur zur Induktion bei, sei es im Wildtypstamm aber auch in der Mutante Rut-C30. Im Gegensatz zum Wildtypstamm, reagiert die Mutante Rut-C30 bei α-Sophorose immer mit einer Chromatinöffnung. Um zwei ähnliche Induktionsprozesse durch zwei unterschiedliche Zucker genauer zu untersuchen, wie es für die Xylanase XYNII der Fall ist, wurden *in vivo* Footprints gemacht. Diese stellen Veränderungen in der Proteinbesetzung an der DNA dar. Als Ergebnis wurden Unterschiede in Protein-DNA-Wechselwirkungen zwischen den Induktionsmodellen gefunden, was auf eine vermutlich unterschiedliche Signaltransduktion zurückgeht. Nicht nur die Xylanaseinduktion ist vom Chromatin beeinflusst, die Chromatinstruktur spielt auch im ‚Upstream'-Genbereich des Transaktivators Xyr1 eine wichtige Rolle. Auf α-Sophorose, wurden höhere *xyr1* Transkripte und eine gleichzeitig erhöhte Chromatinzugänglichkeit gemessen. Im Gegensatz zu *xyr1* und den Xylanasen, zeigten beide Zellulase-kodierende Gene *cbh1* und *cbh2* keine Chromatinöffnung bei α-Sophorose auf.

Im letzten Teil der Arbeit wurde auf die partielle Deletion von Cre1 in der Mutante Rut-C30 eingegangen. Daraus ergibt sich, wie bereits bekannt, die fehlende Katabolitrepression auf D-Glukose in Rut-C30. Mechanistisch gesehen, ist die verkürzte Version von Cre1 (hier Cre1-96 genannt) bisher einer vollständigen Abwesenheit des Repressors Cre1 gleichgesetzt worden. Die Transkript- und Chromatinanalysen zeigten jedoch, dass sich Cre1-96 von einer vollständigen Deletion von Cre1 unterscheidet. Im Gegensatz zur vollständigen Deletion, erhöht Cre1-96 die Zellulaseaktivität, indem es eine offenere Chromatinstruktur in den ‚Upstream'-Bereichen der Zellulasegenen (*cbh1* und c*bh2*) und des Transaktivators Xyr1 verursacht, was mit erhöhtem Transkripten der jeweiligen Gene korreliert. Weiters reguliert Cre1-96 einen potentiell neuen Transkriptionfaktor, der womöglich auf die Umstruktuierung des Chromatins Einfluss nimmt.

Abstract

The filamentous fungus *Trichoderma reesei* is a natural degrader of plant-based biomass. It secretes various hydrolytic enzymes, which act on the plant cell wall's main components, cellulose and hemicellulose. Thereby, the fungus has access to low molecular sugars as nutrients derived from complex polysaccharides. In response to different (sugar) stimuli, *T. reesei* adapts its regulatory circuits and thus the secreted, enzymatic profile. In the presence of D-glucose, an easily-to-metabolize sugar, *T. reesei* undergoes carbon catabolite repression (CCR) of its hydrolytic enzymes. The uptake of such sugars is prioritized and the energy is put into maintance and biomass gain of the fungus. Especially industry was facing here a main bottleneck in cellulase and hemicellulase production. To circumvent the CCR, strain improvement strategies employed random mutagenesis and screenings to create the mutant Rut-C30. The nowadays used industrial *T. reesei* strains are derived from the mutant Rut-C30. This means that they have a partly similar genetic background. The most important characteristics of Rut-C30 are the release of CCR and the increased amount of cellulolytic enzymes. It is still not clear, which exact genetic trait is responsible for the hypercellolytic Rut-C30 phenotype.

The production of the hydrolytic enzymes is regulated to a great extent by the transactivator Xyr1 and the catabolite repressor protein Cre1. Both transcription factors act in a carbon source dependent manner. So far, a lot is known about the interplay between Cre1 and Xyr1 and the impact on cellulase and xylanase expression. However, it has to be considered that the fungal (as any other eukaryotic) DNA is condensed by histones, leading to the formation of nucleosomal arrays along the DNA. By that, the access is modulated for DNA approaching factors (e.g. transcription factors, chromatin remodelers). Together, the binding of transcription factors and the DNA accessibility regulate gene expression. Gathered knowledge about both, can be used for further strain improvements.

This thesis revealed that the DNA accessibility has an impact on cellulase and xylanase expression. Additionally, the effectors of DNA accessibility are either a change in chromatin or the binding of transcription factors, such as Cre1. Transcriptional analysis and chromatin studies showed that the both inducers, D-xylose and α-sophorose, are involved in a chromatin-related induction mechanism of xylanases in the wild-type strain and the mutant Rut-C30. In contrast to the wild-type, an chromatin opening is always observed on α-sophorose in Rut-C30. To distinguish the induction processes by two different inducers, as it is the case for the xylanase XYNII on α-sophorose and D-xylose, changes in protein-binding

to specific DNA-binding sites were monitored by *in vivo* footprinting. This result showed that differences in protein-DNA interactions are inducer dependent and the signalling might be different too. In addition to the xylanase-encoding genes, the DNA accessibility was also investigated in the upstream regulatory region of *xyr1* and of both main cellulases *cbh1* and *cbh2*. In case of *xyr1*, an increased DNA accessibility was found to be a result of an opening in chromatin and led to higher *xyr1* transcript levels upon induction by α-sophorose. In contrast to *xyr1*, the *cbh1* and *cbh2* upstream regulatory regions did not show any chromatin opening in the presence of the inducer α-sophorose.

Finally, the thesis focuses on the partial deletion of Cre1 in Rut-C30. Mechanistically, the partial deletion was equated with a full deletion of Cre1. Transcriptional and chromatin analyses showed that the truncated version of Cre1 (Cre1-96) outcompetes a full deletion of Cre1 in cellulolytic performance. Additionally, Cre1-96 contributes to a more accessible chromatin in the upstream regulatory regions of *cbh1*, *cbh2* and *xyr1* than the full deletion, which results in higher transcript levels of those genes. Last but not least, Cre1-96 influences a helicase-like transcription factor (encoded by *htf1*), which might be involved in chromatin remodelling.

Introduction

All kinds of fungi are represented in different habitats such as soil, water and air. Hence, they have been an essential part of our environment and are a part of our daily lives. The wide spectrum of different fungi brought versatile applications; some of which were used already in antiquity. The employment of filamentous fungi such as *Penicillium* gained high importance in the 1920'ies and revolutionized the medical area until now (Fleming 1929). But not only medicine benefited from fungi. Fungal derived products range from plastics, cosmetics to bulk chemicals such as organic acids (e.g. citric acid) and enzymes. Great attention was drawn to filamentous fungi due to their potential to produce enzymes used in lignocellulosic bioethanol production as a non-fossil derived fuel. The World Energy Council (WEC) calculated the primary energy consumption as a yearly average of 12 billion tons coal equivalent worldwide. The steady increase in the world's population (10 billion people by 2050 according to the United Nations) would demand 24 billion tonnes coal equivalent per year. There is definitely the need for alternatives based on plant biomass, since society has to face depletion of fossil resources, up-going oil prices and the environmental impact of fossil fuels.

Bioconversion of plant-derived biomass shows a great potential to cope with those problems. Wheat straw is a non-food lignocellulosic waste product (approximately 350 million tons worldwide per year (Saini et al. 2015)) and consists of cellulose, hemicellulose and lignin. Cellulose is the most abundant biopolymer in plants, followed by hemicellulose and lignin. Lignin is rigid and highly diverse in its phenolic compounds. To access lignin, physical treatment combined with oxidative enzymatic reactions are necessary (reviewed in (Sánchez 2009)). Cellulose and hemicellulose are degraded enzymatically by cellulases and hemicellulases of various fungal species (reviewed in (Dashtban et al. 2009)).

The filamentous ascomycete *Trichoderma reesei* is an industrially used cellulase and hemicellulase producer. Its hydrolytic enzyme system reacts tightly coordinated to different carbohydrate stimuli in the environment. The cellulolytic subset is induced by cellulose, cellobiose, lactose and α-sophorose (Ilmén et al. 1997). Whereas the main xylanases are induced by the presence of xylan, D-xylose, xylobiose and (at least one of them) also by α-sophorose (Zeilinger et al. 1996, Würleitner et al. 2003). α-Sophorose is interesting in two aspects. Up to now, it is the most potent inducer of cellulases in *T. reesei* (Sternberg & Mandels 1979). On the downside though, it is very costly to use in an industrial scale. It is

naturally produced by a transglycosylation of cellobiose, catalysed by *T. reesei's* β-glucosidases BGLI and BGLII (Fowler & Brown 1992, Mach et al. 1995, Saloheimo et al. 2002). A concentration-dependent induction of the xylanases is observed for D-xylose (Mach-Aigner et al. 2010). High concentrations lead to a repression of xylanase expression, whereas low amounts induce the xylanolytic enzyme system. However, the amount of enzymes secreted naturally does not satisfy industrial purposes. As the demand on large enzyme quantities increased, the field of strain improvement emerged.

The induction by different carbohydrates is one crucial aspect of the whole induction system, but equally important are intracellular mediators of those external signals. A key achievement in *T. reesei* strain engineering was the identification of transcription factors regulating the hydrolytic enzyme production. There are several so far (e.g. Ace1, Ace2, Ace3, Xpp1, Hap2/3/5 (Aro et al. 2001, Zeilinger et al. 2001, Aro et al. 2003, Häkkinen et al. 2014, Derntl et al. 2015)), but the focus of this thesis will be on the two main regulators and their mode of action. The two main mediators are the activator Xyr1 (Stricker et al. 2006) and the repressor Cre1 (Strauss et al. 1995). Xyr1 is the main activator of the expression of hydrolytic enzymes in *T. reesei* (Stricker et al. 2006). It was identified by sequence homologies to XlnR in *A. niger* (van Peij et al. 1998). Xyr1 belongs to the zinc binuclear (Zn_2Cys_6) cluster protein and binds to 5'-GGCWWW- 3' motifs to its target genes (Furukawa et al. 2009). In context to the hydrolytic enzyme-encoding genes, the most prominent targets of Xyr1 are the cellulase-encoding genes *cbh1*, *cbh2*, *egl1* and *bgl1* and the xylanase-encoding genes *bxl1*, *xyn1* and *xyn2* (Stricker et al. 2006). Interestingly, the transcription profiles of *cbh1* and *cbh2* are co-regulated with the *xyr1* transcription (Derntl et al. 2013). The transcription of the xylanase-encoding genes *xyn1* and *xyn2* are dependent on Xyr1, but not solely. The regulatory fine-tuning of *xyn1* and *xyn2* transcription is achieved by gene-specific factors such as Ace1, Ace2, Xpp1 and Hap2/3/5 (Würleitner et al. 2003, Rauscher et al. 2006). The transcription of *xyr1* occurs at a basal level under non-inducing conditions and is repressed on D-glucose (Mach-Aigner et al. 2008). α-Sophorose, however, induces the *xyr1* transcription (Derntl et al. 2013) and in addition leads to an increase in the ratio of nuclear localized Xyr1 compared to cytosolic localized Xyr1 (Lichius et al. 2014). The activating role of Xyr1 is not restricted to the expression of hydrolytic enzymes. It is also involved in the expression of enzymes involved in the D-xylose and lactose metabolism, by influencing directly the D-xylose reductase activity (Stricker et al. 2006, Stricker et al. 2007).

In contrast to Xyr1, Cre1 is the main repressor of cellulase and hemicellulase expression. Cre1 mediates the carbon catabolite repression (CCR), a highly conserved mechanism amongst different species. CCR is triggered by high concentrations of easily metabolizable sugars, such as D-glucose or D-xylose. As a consequence, more complex substrates are not metabolized until D-glucose or D-xylose will have been depleted and the hydrolytic system remains shut down until then. Cre1 was identified by sequence homology of CreA in *A. niger/nidulans* and Mig1p in *S. cerevisiae* (Nehlin & Ronne 1990). Like its homolog, Mig1p, Cre1 is a C_2H_2 zinc finger protein and translocates into the nucleus in the presence of D-glucose (De Vit et al. 1997, Lichius et al. 2014). Moreover, it gets phosphorylated in the presence of D-glucose. Upon phosphorylation, Cre1 is able to bind to 5'-SYGGRG- 3' motifs within the upstream regulatory regions of its target genes and exerts its full active form as a carbon catabolite repressor (Cziferszky et al. 2002). For industrial cellulase production, CCR is a hindrance, as Cre1 represses the transcription of the genes encoding for the main activator Xyr1 and also for one of the two main cellulases, CBHI (encoded by *cbh1*), and for the xylanase, XYNI (encoded by *xyn1*). Strain improvement strategies employed random mutagenesis to yield a hypercellulolytic strain, called Rut-C30 (Montenecourt & Eveleigh 1979). This strain achieves enzyme yields up to 20 mg/mL and qualifies therefore for industrial purposes. Notably, most nowadays used industrial *T. reesei* strains are derived from the mutant Rut-C30. From a genetic point of view, it shows several chromosome rearrangements (Mäntylä et al. 1992), including a 85 kb deletion (Seidl et al. 2008) and a partial deletion of Cre1 (Ilmén et al. 1996) as the main features. Latter leads to de-repression of cellulase expression on D-glucose.

Furthermore, it has to be considered, that eukaryotic DNA is packed together with histones to chromatin, which adds an additional layer to the gene regulation. Chromatin consists of nucleosomes, a DNA-protein unit, containing 147 bp of DNA wrapped around an octamer of histone proteins (Kornberg 1974). Two distinct forms of chromatin can be distinguished, exemplary depending on the frequency and density of nucleosomes along the DNA: euchromatin and heterochromatin. Euchromatin is a more open form of chromatin, which allows transcription factors or other proteins to access the DNA. In contrast to that, heterochromatin is associated with a very densely packed chromatin. The dense packaging is achieved by the recruitment of heterochromatin-associated proteins or histone-modifying enzymes (e.g. heterochromatin protein 1 in fission yeast (Nonaka et al. 2001)). As both states are in transition to each other, the chromatin is under constant reconstruction. In brief, the

gene expression can be regulated in two ways: firstly by the chromatin accessibility and secondly, by the binding of transcription factors.

Up to now, only a few studies have been conducted to investigate the chromatin-based gene regulation in *T. reesei*. A contribution to the local nucleosomal structure of the cellulase-encoding genes requires Cre1, particularly in *cbh1*, and the Hap2/3/5 complex in *cbh2* (Zeilinger et al. 2003, Ries et al. 2014). For the xylanase-encoding genes, a nucleosomal model was proposed only for *xyn2* (Würleitner et al. 2003). In *xyn2*, a nucleosome free region was found spanning across the TATA box and this region remains accessible under inducing and non-inducing conditions (Würleitner et al. 2003). However, chromatin is more than just nucleosomes. Transcription factor binding sites are also hot spots to examine changes in their binding behaviour. As already mentioned, Cre1 does have an effect on nucleosome arrangement. But it is not known, if other transcription factors have also an effect on changes in protein-DNA interactions in their target genes. These changes in protein-DNA interactions could contribute to a chromatin-related gene regulation besides the nucleosomal structure.

Aims

This thesis deals with the DNA accessibility of cellulase and hemicellulase-encoding genes in different *T. reesei* strains.

The experimental set ups were performed on different carbon sources (D-glucose as a repressing carbon source, D-xylose and α-sophorose as inducing conditions) in the wild-type strain QM6a and in the mutant strain Rut-C30, which has an industrial relevance. The chromatin-related studies are of great importance, because gene regulation is not restricted solely to transcription factors.

First, the impact of the chromatin on the xylanase expression was investigated. Various inducer molecules achieve the induction of xylanase expression, but some exert a greater induction potential than others. Here, it was investigated how the two inducing substances, D-xylose and α-sophorose contribute to the xylanase expression in regard to the chromatin accessibility in the wild-type strain and in the mutant Rut-C30. A special focus was on the alterations in protein-DNA interactions across the upstream regulatory regions of the *xyn1* and *xyn2* promoters and on changes of the pattern depending on the inducer applied.

As the main activator of cellulase and xylanase expression, Xyr1 is an obvious target for transcriptional and further chromatin studies. So far, it is quite possible that Xyr1 acts on the DNA accessibility.

As a second aim, this thesis covers the impact of Xyr1 on chromatin and the differences in protein-DNA interaction patterns in the upstream regions of the transactivator Xyr1 itself and for the cellulase-encoding genes. Chromatin accessibility studies (CHART-PCR) and transcript analysis are required to elucidate the context of chromatin and transcript profiles of *xyr1*, *cbh1* and *cbh2*.

Finally, the truncated version of Cre1 was subject of the last part of this thesis. The partial deletion of Cre1 is present in most industrial *T. reesei* strains, including Rut-C30. Although it is only partially deleted, the function of the truncated Cre1 is compared to a full deletion of Cre1 and in both cases it is regarded as a Cre1-negative background. It remains still obscure to what extent the partial deletion of Cre1 might be responsible for the increased production of cellulolytic enzymes in Rut-C30. Both, transcriptional and chromatin-related information is required to examine the impact of DNA accessibility on cellulase activity. Furthermore, *in vivo* footprinting analyses and EMSA experiments investigated the changes on Cre1 binding sites in Rut-C30 compared to the wild-type strain QM6a.

Conclusions

The stated aims were properly addressed in the three publications included in this thesis. The inducer-dependent profiles of protein-DNA interactions across the *xyn1* and *xyn2* upstream regions were obtained by chromatin studies and *in vivo* footprinting. Moreover, the context of chromatin and transcription was shown for *xyr1* and its targets *cbh1* and *cbh2*. And finally, the partial deletion of Cre1 in Rut-C30 was further investigated.

The xylanase induction is achieved by two different inducers, namely D-xylose and α-sophorose. Chromatin studies and transcription analysis showed that *xyn1* is strongly induced by D-xylose, but it does not involve a chromatin opening. When it comes to *xyn2* transcription, D-xylose and α-sophorose induce in a similar fashion. These similarities are reflected in the transcripts and the chromatin status within an upstream regulatory region in the wild type and mutant Rut-C30. However, the *in vivo* footprinting showed that the α-sophorose induction does not involve additional DNA-interacting proteins. This suggests that the signalling pathway on α-sophorose and D-xylose are different and might involve two (partly) distinct induction machineries for *xyn2*.

Additionally, the chromatin accessibility is generally higher in Rut-C30 than in the wild-type strain for the xylanase-encoding genes *xyn1* and *xyn2*. A similar trend was observed for the upstream regulatory region in *xyr1*. The higher *xyr1* transcript is related to a higher chromatin accessibility in both strains under inducing conditions (α-sophorose). So far, the xylanase-encoding genes and the *xyr1* promoter became targets of chromatin accessibility changes. However, the chromatin studies revealed that the DNA accessibility plays only a secondary role in cellulase expression. The cellulase induction is primarily dictated by the levels of Xyr1 available.

Lastly, the truncated form of Cre1 (Cre1-96) contributes to the enhanced cellulase production in Rut-C30. Due to the partial deletion, the remaining protein Cre1-96 is left with only one zinc finger. Interestingly, Cre1-96 is still able to bind DNA independently of any carbon source. This suggests, that the repressor protein Cre1 might have converted to a putative activator in Rut-C30. The activating effect of Cre1-96 was shown in an enhanced cellulase activity and a chromatin opening in the upstream regulatory regions of the cellulase-encoding genes and the transactivator *xyr1*. The mechanism of the chromatin opening seems to involve a chromatin-remodelling factor (encoded by *htf1*), whose expression is Cre1-96 dependent.

References for Introduction

Aro N, Ilmén M, Saloheimo A, Penttilä M. 2003 – ACEI of Trichoderma reesei is a repressor of cellulase and xylanase expression. Applied and environmental Microbiology 69, 56-65.

Aro N, Saloheimo A, Ilmén M, Penttilä M. 2001 – ACEII, a novel transcriptional activator involved in regulation of cellulase and xylanase genes of *Trichoderma reesei*. The Journal of biological chemistry 276, 24309-24314.

Cziferszky A, Mach RL, Kubicek CP. 2002 – Phosphorylation positively regulates DNA binding of the carbon catabolite repressor Cre1 of *Hypocrea jecorina* (*Trichoderma reesei*). J Biol Chem 277, 14688-14694.

Dashtban M, Schraft H, Qin W. 2009 – Fungal Bioconversion of Lignocellulosic Residues; Opportunities & Per- spectives. International Journal of Biological Sciences 5, 578-595.

De Vit M, Waddle J, Johnston M. 1997 – Regulated nuclear translocation of Mig1 glucose repressor. Molecular Biology of the Cell 8, 1603-1618.

Derntl C, Gudynaite-Savitch L, Calixte S, White T, Mach RL, Mach-Aigner AR. 2013 – Mutation of the Xylanase regulator 1 causes a glucose blind hydrolase expressing phenotype in industrially used *Trichoderma* strains. Biotechnology for biofuels 6, 62.

Derntl C, Rassinger A, Srebotnik E, Mach RL, Mach-Aigner AR. 2015 – Xpp1 regulates expression of xylanases but not of cellulases in *Trichoderma reesei*. Biotechnology for biofuels 8, 11.

Fleming A. 1929 – On the Antibacterial Action of Cultures of a *Penicillium*, with Special Reference to their Use in the Isolation of *B. influenzæ*. Br J Exp Pathol 10, 226-236.

Fowler T, Brown RD, Jr. 1992 – The *bgl1* gene encoding extracellular beta-glucosidase from *Trichoderma reesei* is required for rapid induction of the cellulase complex. Mol Microbiol 6, 3225-3235.

Furukawa T, Shida Y, Kitagami N, Mori K, Kato M, Kobayashi T, Okada H, Ogasawara W, Morikawa Y. 2009 – Identification of specific binding sites for XYR1, a transcriptional activator of cellulolytic and xylanolytic genes in *Trichoderma reesei*. Fungal Genetics and Biology 46, 564-574.

Häkkinen M, Valkonen MJ, Westerholm-Parvinen A, Aro N, Arvas M, Vitikainen M, Penttilä M, Saloheimo M, Pakula TM. 2014 – Screening of candidate regulators for cellulase and hemicellulase production in *Trichoderma reesei* and identification of a factor essential for cellulase production. Biotechnology for biofuels 7.

Ilmén M, Saloheimo A, Onnela ML, Penttilä ME. 1997 – Regulation of cellulase gene expression in the filamentous fungus *Trichoderma reesei*. Appl Environ Microbiol 63, 1298-1306.

Ilmén M, Thrane C, Penttilä M. 1996 – The glucose repressor gene *cre1* of *Trichoderma*: isolation and expression of a full-length and a truncated mutant form. Molecular and General Genetics 251, 451-460.

Kornberg R. 1974 – Chromatin structure: A repeating unit of histones and DNA. Science 184, 868-871.

Lichius A, Seidl-Seiboth V, Seiboth B, Kubicek CP. 2014 – Nucleo-cytoplasmic shuttling dynamics of the transcriptional regulators XYR1 and CRE1 under conditions of cellulase and xylanase gene expression in *Trichoderma reesei*. Molecular Microbiology 94, 1162-1178.

Mach RL, Seiboth B, Myasnikov A, Gonzalez R, Strauss J, Harkki AM, Kubicek CP. 1995 – The *bgl1* gene of *Trichoderma reesei* QM 9414 encodes an extracellular, cellulose-inducible beta-glucosidase involved in cellulase induction by sophorose. Mol Microbiol 16, 687-697.

Mach-Aigner AR, Pucher ME, Mach RL. 2010 – D-Xylose as a repressor or inducer of xylanase expression in *Hypocrea jecorina* (*Trichoderma reesei*). Appl Environ Microbiol 76, 1770-1776.

Mach-Aigner AR, Pucher ME, Steiger MG, Bauer GE, Preis SJ, Mach RL. 2008 – Transcriptional regulation of *xyr1*, encoding the main regulator of the xylanolytic and cellulolytic enzyme system in *Hypocrea jecorina*. Appl Environ Microbiol 74, 6554-6562.

Mäntylä AL, Rossi KH, Vanhanen SA, Penttilä ME, Suominen PL, Nevalainen KM. 1992 – Electrophoretic karyotyping of wild-type and mutant *Trichoderma longibrachiatum* (*reesei*) strains. Curr Genet 21, 471-477.

Montenecourt BS, Eveleigh DE. 1979. Selective Screening Methods for the Isolation of High Yielding Cellulase Mutants of *Trichoderma reesei*. In: Brown RD, Jurasek L, editors. Hydrolysis of Cellulose: Mechanisms of Enzymatic and Acid Catalysis. Washington, DC: American Chemical Society. p 289-301.

Nonaka N, Kitajima T, Yokobayashi S, Xiao G, Yamamoto M, Grewal SIS, Watanabe Y. 2001 – Recruitment of cohesin to heterochromatic regions by Swi6/HP1 in fission yeast. Nature Cell Biology 4, 89-93.

Rauscher R, Würleitner E, Wacenovsky C, Aro N, Stricker AR, Zeilinger S, Kubicek CP, Penttilä M, Mach RL. 2006 – Transcriptional regulation of *xyn1*, encoding xylanase I, in *Hypocrea jecorina*. Eukaryotic Cell 5, 447-456.

Ries L, Belshaw NJ, Ilmén M, Penttilä ME, Alapuranen M, Archer DB. 2014 – The role of CRE1 in nucleosome positioning within the *cbh1* promoter and coding regions of *Trichoderma reesei*. Applied Microbiology and Biotechnology 98, 749-762.

Saini JK, Saini R, Tewari L. 2015 – Lignocellulosic agriculture wastes as biomass feedstocks for second-generation bioethanol production: concepts and recent developments. 3 Biotech 5, 337-353.

Saloheimo M, Kuja-Panula J, Ylosmaki E, Ward M, Penttilä M. 2002 – Enzymatic properties and intracellular localization of the novel *Trichoderma reesei* beta-glucosidase BGLII (cel1A). Appl Environ Microbiol 68, 4546-4553.

Sánchez C. 2009 – Lignocellulosic residues: Biodegradation and bioconversion by fungi. Biotechnology Advances 27, 185-194.

Seidl V, Gamauf C, Druzhinina IS, Seiboth B, Hartl L, Kubicek CP. 2008 – The *Hypocrea jecorina* (*Trichoderma reesei*) hypercellulolytic mutant RUT C30 lacks a 85 kb (29 gene-encoding) region of the wild-type genome. BMC Genomics 9, 327.

Sternberg D, Mandels GR. 1979 – Induction of cellulolytic enzymes in *Trichoderma reesei* by sophorose. J Bacteriol 139, 761-769.

Strauss J, Mach RL, Zeilinger S, Hartler G, Stoffler G, Wolschek M, Kubicek CP. 1995 – Cre1, the carbon catabolite repressor protein from *Trichoderma reesei*. FEBS Letters 376, 103-107.

Stricker AR, Grosstessner-Hain K, Würleitner E, Mach RL. 2006 – Xyr1 (xylanase regulator 1) regulates both the hydrolytic enzyme system and D-xylose metabolism in *Hypocrea jecorina*. Eukaryotic Cell 5, 2128-2137.

Stricker AR, Steiger MG, Mach RL. 2007 – Xyr1 receives the lactose induction signal and regulates lactose metabolism in *Hypocrea jecorina*. FEBS Lett 581, 3915-3920.

van Peij NN, Visser J, de Graaff LH. 1998 – Isolation and analysis of *xlnR*, encoding a transcriptional activator co- ordinating xylanolytic expression in *Aspergillus niger*. Mol Microbiol 27, 131-142.

Würleitner E, Pera L, Wacenovsky C, Cziferszky A, Zeilinger S, Kubicek CP, Mach RL. 2003 – Transcriptional regulation of *xyn2* in *Hypocrea jecorina*. Eukaryotic Cell 2, 150-158.

Zeilinger S, Ebner A, Marosits T, Mach R, Kubicek CP. 2001 – The *Hypocrea jecorina* HAP 2/3/5 protein complex binds to the inverted CCAAT-box (ATTGG) within the *cbh2* (cellobiohydrolase II-gene) activating element. Mol Genet Genomics 266, 56-63.

Zeilinger S, Mach RL, Schindler M, Herzog P, Kubicek CP. 1996 – Different inducibility of expression of the two xylanase genes *xyn1* and *xyn2* in *Trichoderma reesei*. Journal of Biological Chemistry 271, 25624-25629.

Zeilinger S, Schmoll M, Pail M, Mach RL, Kubicek CP. 2003 – Nucleosome transactions on the *Hypocrea jecorina* (*Trichoderma reesei*) cellulase promoter *cbh2* associated with cellulase induction. Molecular Genetics and Genomics 270, 46-55.

Peer reviewed publications

Chapter 1

Peer-reviewed publication: ‚Impact of xylanase expression-inducing compounds on DNA accessibility in *Trichoderma reesei'* published in Mycosphere 8(3), 432-444 (2017)

Authors' Contributions

The author of this thesis, Alice Rassinger, performed the *in vivo* footprinting assays, participated in the execution of the chromatin accessibility real-time PCRs (CHART-PCRs) and quantitative PCRs (qPCRs) and drafted the manuscript.

Mycosphere 8(3) 432-444 (2017) www.mycosphere.org ISSN 2077 7019

Article – special issue
Doi 10.5943/mycosphere/8/3/5

Impact of xylanase expression-inducing compounds on DNA accessibility in *Trichoderma reesei*

Rassinger A[1,†], Mello-de-Sousa TM[1,†], Regnat K[1], Derntl C[1], Mach RL[1] and Mach-Aigner AR[1]

[1] *Institute of Chemical Engineering, Department for Biotechnology and Microbiology, TU Wien, Vienna, Austria.* alice.rassinger@tuwien.ac.at, thiago.mello@tuwien.ac.at, katharina.regnat@tuwien.ac.at, christian.derntl@tuwien.ac.at, robert.mach@tuwien.ac.at, astrid.mach-aigner@tuwien.ac.at
[†]*Equal contributors*

Rassinger A, Mello-de-Sousa TM, Regnat K, Derntl C, Mach RL, Mach-Aigner 2016 – Impact of xylanase expression-inducing compounds on DNA accessibility in *Trichoderma reesei*. Mycosphere 8(3) 432–444, Doi 10.5943/mycosphere/8/3/5

Abstract

The ascomycete *Trichoderma reesei* produces industrially applied plant cell wall-degrading enzymes. The two major xylanases XYNI (encoded by *xyn1)* and XYNII (encoded by *xyn2*) are amongst those enzymes. The transactivator Xyr1, the repressor Cre1, and gene-specific transcription factors regulate the expression of both xylanases. The inducing compounds D-xylose and sophorose trigger the expression of the xylanases, however, to different extents. D-glucose causes carbon catabolite repression (CCR) mediated by Cre1, which leads to a down-regulation of expression of both. Apart from transcription factors, DNA packaging adds an important layer to the regulation of the production of xylanolytic enzymes. In this study the chromatin status in two upstream regulatory regions (URRs) of the *xyn1* and *xyn2* genes and the transcript levels were investigated in the wild-type strain QM6a and the hypercellulolytic mutant Rut-C30. This analysis demonstrated more open chromatin and higher transcript levels in both strains and genes under at least one of the two inducing conditions. Additionally, a generally more open chromatin could be observed in Rut-C30 independent of the carbon source that was accompanied by elevated transcript levels. *In vivo* footprinting analyses demonstrated that protein-DNA interactions differ between D-xylose compared to D-glucose in both strains. In addition, different DNA occupancies were observed in the URR of *xyn2* in dependency of the applied inducer. Obviously, the usage of a certain inducer influences the final promoter architecture.

Key words – Chromatin – D-xylose – Inducers – sophorose – *Trichoderma reesei* – xylanases

Introduction

Trichoderma reesei (teleomorph *Hypocrea jecorina* (Kuhls et al. 1996)) is a filamentous ascomycete, which exerts a saprotrophic lifestyle. It gains its nutrients by degradation of plant cell wall material. For this purpose, it secretes various cellulases and hemicellulases to break down complex polysaccharides. Synergistic action of *T. reesei's* secreted enzyme cocktail leads to a degradation of the plant biomass.

The two main cellobiohydrolases CBHI (encoded by *cbh1*) and CBHII (encoded by *cbh2*) (Teeri 1983) act on cellulose, the most abundant polysaccharide in nature. However,

plant cell walls are not only made of cellulose. Hemicelluloses add high variability to the structure of plant cell walls by their side chains. Xylan is the most abundant polysaccharide amongst the hemicelluloses. *T. reesei* secretes two major endo-β-1,4-xylanases to degrade xylan. These are XYNI (encoded by *xyn1*) and XYNII (encoded by *xyn2*) (Törrönen et al. 1992). Apart from their function in nature, endo-β-1,4-xylanases are widely used in industrial applications (Viikari et al. 1994).

On the transcriptional level, both xylanases share common regulatory mechanisms. Transcriptional regulation is basically dependent on the interplay of the Xylanase regulator 1 (Xyr1) (Stricker et al. 2006) and the carbon catabolite repressor Cre1 (Strauss et al. 1995). Xyr1 is a GAL4-like transactivator and binds to the six nucleotide sequence 5'-GGC(T/A)$_3$-3' (Furukawa et al. 2009). This motif occurs typically as repeats in Xyr1-target promoters. For instance, in the *xyn1* promoter, a regulatory element was described to be functional *in vivo* that contains two Xyr1-binding sites arranged as an inverted repeat. Mutation of the Xyr1-binding sites within this element resulted in a loss of *xyn1* expression (Rauscher et al. 2006). *Xyr1* itself is transcribed at a low basal level on most carbon sources and is induced by the transglycosylation product sophorose (Derntl et al. 2013). In contrast to cellulase-encoding genes, transcription levels of *xyn1* and *xyn2* do not respond directly to an increased transcription level of *xyr1*. The authors suggested that the regulation of xylanase expression involves further regulatory mechanisms (Derntl et al. 2013).

Cre1 is a C_2H_2 zinc finger protein, it binds to a 5′-SYGGRG-3′ binding motif (Strauss et al. 1995), and it mediates carbon catabolite repression (CCR) in the presence of readily metabolizable carbon sources, such as D-glucose. Cre1 acts directly on the transcription of its target genes, *e.g. cbh1* (Ilmén et al. 1998), *xyn1* (Mach et al. 1996), and *xyr1* (Mach-Aigner et al. 2008). Consequently, CCR is acting on two different hierarchical levels, *i.e.* indirectly, by repressing the expression of the main activator Xyr1, and directly, by binding to the upstream regulatory regions (URRs) of the respective target genes. As a third common transcription factor, the CCAAT-box binding protein complex Hap2/3/5 plays a role in the expression of *xyn1* and *xyn2* (Würleitner et al. 2003, Rauscher et al. 2006).

In addition, gene-specific transcription factors are involved in regulation of *xyn1* and/or *xyn2* transcription. For instance, the Activator of cellulases 1 (Ace1) (Aro et al. 2003) acts as a repressor of *xyn1* expression (Rauscher et al. 2006). The Activator of cellulases 2 (Ace2) (Aro et al. 2001) and the Xylanase promoter-binding protein 1 (Xpp1) (Mach-Aigner et al. 2010, Derntl et al. 2015) influence *xyn2* transcription (Würleitner et al. 2003, Stricker et al. 2008a, Derntl et al. 2015). Xpp1 exerts a repressive function in regard to transcriptional regulation, whereas Ace2 rather acts as an activator. Although both xylanase-encoding genes share common transcription factors, their regulation of gene expression varies in terms of their response to available carbohydrates. For *xyn2*, a low basal transcription level is observed even under repressing conditions (*e.g.* on D-glucose) (Derntl et al. 2013). Induction of *xyn2* expression occurs on sophorose, xylobiose, and in the presence of D-xylose (Zeilinger et al. 1996, Würleitner et al. 2003). On the other hand, *xyn1* is subjected to CCR and is therefore completely shut off under repressing conditions (Mach et al. 1996). Induction of *xyn1* expression is mainly achieved on D-xylose (Zeilinger et al. 1996). The reasons for the different induction behaviour of the two xylanases are not fully understood yet.

Additionally to transcription factors, chromatin contributes to the regulation of transcription. In a recent study, it was shown that chromatin packaging plays a role in the regulation of transcription of the cellulase-encoding genes *cbh1* and *cbh2* (Ries et al. 2014, Mello-de-Sousa et al. 2016). Further, in an earlier study, it was reported that in the absence of Xyr1, the chromatin status of cellulase-encoding genes got denser and was accompanied by a decreased expression (Mello-de-Sousa et al. 2015). When the cellulase expression and the chromatin status are pulled together, the industrially important strain Rut-C30 has to be mentioned. Rut-C30 was generated by 3 mutagenesis steps starting from QM6a as the

originate strain (Montenecourt & Eveleigh 1979a, Montenecourt & Eveleigh 1979b). This yielded the high cellulase-producing strain with a phenotype released from CCR. Importantly, Rut-C30 bears a truncated version of Cre1 (Cre1-96), which seems to contribute to a more open chromatin status (Mello-de-Sousa et al. 2014). Moreover, MNaseI digestion of the *cbh1* and *cbh2* promoter were performed. It was found that the structural gene of *cbh1* shows a complete loss of positioned nucleosomes in Rut-C30 despite the tested carbon source (Ries et al. 2014). Whereas in *cbh2* both, structural gene and the region located upstream of the start codon showed a full depletion of nucleosomes under repression and inducing conditions (Zeilinger et al. 2003). In terms of xylanase production, Rut-C30 is also relevant for industrial purposes considering the release of *xyn1* expression from CCR. The extent of inducibility of *xyn1* and *xyn2* expression was found to be different on D-xylose compared to sophorose in Rut-C30 (Derntl et al. 2013). However, a possible influence of the chromatin status on the expression of xylanases has not been investigated yet (as it was done for the cellulases).

In this study, we investigated the chromatin status and the protein-DNA interactions in the URRs of both xylanase-encoding genes. A special focus was the comparative analysis of the two different inducing conditions (D-xylose, sophorose) in relation to a repressing (D-glucose) condition. To this end, CHART-PCR, qPCR, and *in vivo* footprinting analyses were performed to investigate two selected regions in the URR of each xylanase-encoding gene in the wild-type strain QM6a and in Rut-C30.

Materials & methods

Fungal strains

The following *T. reesei* strains were used throughout this study: *T.reesei* QM6a (ATCC 13631) is the wild-type strain and is referred to as reference strain. The other strain of interest is the hypercellulolytic strain Rut-C30 (ATCC 56765), which is the common ancestor of most *T.reesei* industrial strains. All strains were maintained on 3 % malt extract agar plates containing 0.1 % (w/v) peptone.

Growth conditions

For carbon source replacement experiments, fungal mycelia were pre-cultured in 1 l Erlenmeyer flasks on a rotary shaker (180 rpm) at 30 °C for 24 h in 250 ml of Mandels-Andreotti (MA) medium (Mandels 1985) containing 1 % (w/v) glycerol as sole carbon source. For inoculation 10^9 conidia per litre (final concentration) were used. Pre-grown mycelia were washed, equally distributed, and resuspended in 20 ml or 100 ml MA media containing 1 % (w/v) D-glucose, 0.5 mM D-xylose, 2 mM sophorose or no carbon source, respectively. Replacement cultures were then incubated on a rotary shaker (180 rpm) at 30 °C for 3 h. Samples were derived from three biological replicates and were pooled before RNA extraction and chromatin digestion.

Analysis of transcript levels

0.01 - 0.03 mg frozen fungal mycelia were homogenized in 1 ml of peqGOLDTriFast DNA/RNA/protein purification system reagent (PEQLAB Biotechnology, Erlangen, Germany) using a FastPrep(R)-24 cell disrupter (MP Biomedicals, Santa Ana, CA, USA). RNA isolation was conducted following the manufacturer's instructions and the concentration was measured using the NanoDrop 1000 (Thermo Scientific, Waltham, US). Synthesis of cDNA from mRNA was carried out using the RevertAidTM H Minus First Strand cDNA Synthesis Kit (Thermo Scientific, Waltham, USA) according to the manufacturer's instructions. Quantitative, reverse transcription PCRs (RT-qPCRs) were performed in a Rotor-Gene Q system (Qiagen, Hilden, Germany). All reactions were performed in triplicates. The reaction mixture had a final volume of 15 µl containing 7.5 µl 2 x iQ SYBR Green Mix (Bio-Rad, Hercules, USA), 100 nM forward and reverse primer, and 2.5 µl cDNA (diluted

1:20). Primer sequences are provided in table 1. Cycling conditions and control reactions were performed as described previously (Steiger et al. 2010). Data normalization using *sar1* and *act* as reference genes, and calculations were performed as published previously (Steiger et al. 2010).

Chromatin accessibility real-time PCR (CHART-PCR)

DNaseI digestions of chromatin and subsequent quantitative PCR (qPCR) analyses were carried out as described before (Mello-de-Sousa et al. 2014). qPCR analyses of the DNaseI-treated samples were performed to measure the relative abundance of DNA of the target regions. PCRs were performed in triplicates in a Rotor-Gene Q system (Qiagen) using the reaction mixture (final volume 20 µl) and the cycling conditions as described before (Mello-de-Sousa et al. 2014). Primer sequences are provided in table 1.

Table 1 Primer sequences and their employment in the study are listed here. All sequences are given in 5' to 3' orientation.

Primer name	Sequence	Employment
epixyn1_1Tr_f	GCACTCCAAGGCCTTCTCCTGTACT	*xyn1* CHART, region −577 to −278
epixyn1_1Tr_r	TAGATTGAACGCCACCCGCAATATC	
epixyn1_3Tr_f	GTCGATATTGCGGGTGGCGTTCAAT	*xyn1* CHART, region −306 to −10
epixyn1_3Tr_r	TTTGTGCGTGTTTTCCTTGAAGTCG	
epixyn2_1Tr_f	GTGCCGATGAGACGCTGCTGAGAAA	*xyn2* CHART, region −527 to −252
epixyn2_1Tr_r	GATATTGCGCCTTGCAACACCATCG	
epixyn2_2Tr_f	CTCGAGACGGCTGAGACAGCAGCAT	*xyn2* CHART, region −311 to −38
epixyn2_2Tr_r	TGTCTTTTGGGCTTGGAGGGGTTGT	
actfw	TGAGAGCGGTGGTATCCACG	RT-qPCR
actrev	GGTACCACCAGACATGACAATGTTG	
sar1fw	TGGATCGTCAACTGGTTCTACGA	
sar1rev	GCATGTGTAGCAACGTGGTCTTT	
xyn1f	CAGCTATTCGCCTTCCAACAC	
xyn1r	CAAAGTTGATGGGAGCAGAAG	
taqxyn2f	GGTCCAACTCGGGCAACTTT	
taqxyn2r	CCGAGAAGTTGATGACCTTGTTC	
xyn1_1 oligo 3 f	[6-FAM]AGCCCCAGCAGAACATGTCGTCGG	*xyn1* footprint, region 1 -869 to -598
xyn1_1 oligo 3 r	[6-FAM] AGGGGCTTCATGTCGGACTTGCGG	
xyn1_2 oligo 3 f	[6-FAM] AGCAGCTACATCTACCAAGACACTCGTGC A	*xyn1* footprint, region 2 -513 to -361
RG72	[6-FAM] GAGGTTGAAAGCGGCTCGTACAGTATCC	
xyn2_1 oligo 3 f	[6-FAM] TGTGATGCTGCTGCTGATGGCTAATCCC	*xyn2* footprint, region 1 -580 to -373
xyn2_1 oligo 3 r	[6-FAM] CTCATCAAGCTTGCCTCGTCTCCGC	
RG131	[6-FAM] CCGTTATTCAGACAATGTATGTGCCGGGC	*xyn2* footprint, region 2 -258 to -73
RG132	[6-FAM] GTTGTTGTGTCTTTTGGGCTTGGAGGGG	

The amount of intact input DNA of each sample was calculated by comparing the threshold values of the PCR amplification plots with a standard curve generated for each primer set using serial dilutions of genomic, undigested DNA. The chromatin accessibility index (CAI) was defined as: CAI = (Dc1+Dc2)/2Ds, where Ds is the amount of intact DNA detected for each target region, and Dc1 and Dc2 are the amounts of intact DNA detected for the promoter regions of *sar1* and *act,* respectively, which were used as reference genes for normalization.

In vivo footprinting analysis

In vivo methylation using dimethyl sulphate (DMS) followed by ligation-mediated PCR was performed as described previously (Gorsche et al. 2013). Primer sequences are provided in table 1. The separation of fragments was performed by capillary gel electrophoresis (Microsynth, Balgach, Switzerland) and results were analysed using the ivFAST program (Gorsche et al. 2013). The ivFAST output data is statistically tested (Student's t-test) within a two-sided 95% confidence interval and gives significantly different values. Landscape visualization of data was generated as described previously (Mello-de-Sousa et al. 2014) and displayed as the protein-DNA interaction index (PDI). The PDI indicates a relative ratio of protein-DNA interactions derived from mycelia incubated on D-xylose or sophorose compared to D-glucose (reference condition) for both strains and regions.

Results and Discussion

Other than by D-xylose, the induction by sophorose always goes along with chromatin opening

To investigate the role of the chromatin status during the induction of the xylanase expression, the wild-type strain QM6a and the strain Rut-C30 (released from CCR) were pre-grown on glycerol and then transferred to the two inducing substances, namely D-xylose and sophorose. Further, D-glucose was used as a repressing carbon source and no carbon source as the reference condition. The fungal mycelia were then subjected to DNaseI digestions and a CHART-PCR assay was employed to determine the chromatin accessibility of the URRs of *xyn1* and *xyn2*. To relate the chromatin accessibility to the transcription profile of both strains, RT-qPCRs of the respective genes (i.e. *xyn1* and *xyn2*) were performed. Two regions for the CHART-PCR of each gene were chosen based on the frequency of occurrence of transcription factor-binding sites in the respective URRs. The chosen regions are depicted in figure 1.

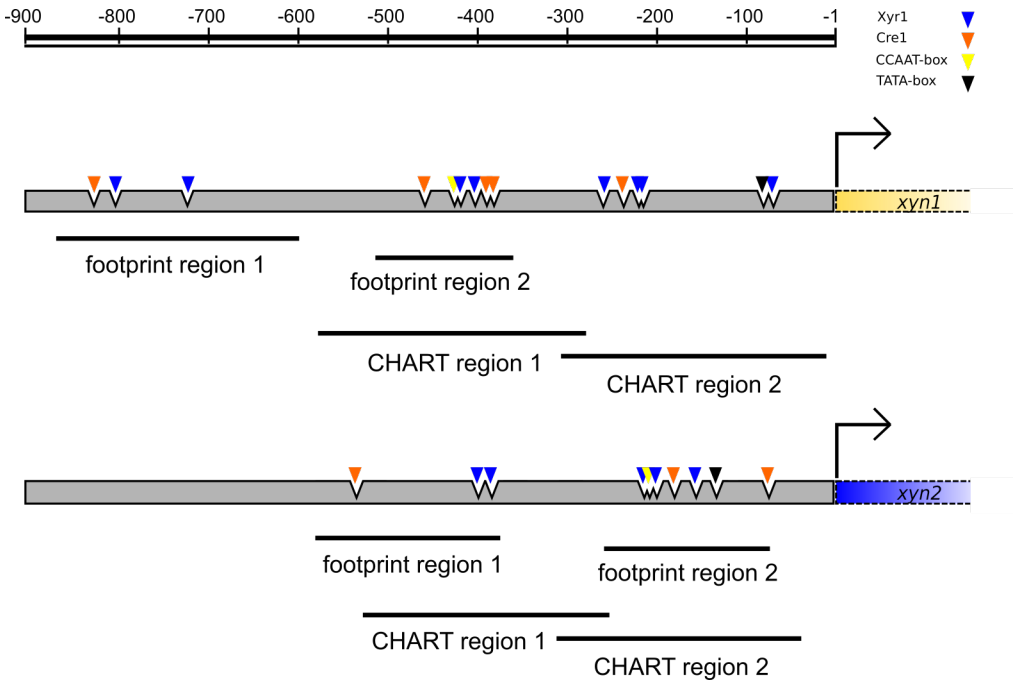

Fig 1 – URRs of *xyn1* and *xyn2* are schematically presented. Grey bars represent URRs of the respective genes. Yellow (*xyn1*) and blue (*xyn2*) bars depict the structural genes. Within the URRs, transcription factor-binding sites are symbolized by coloured triangles: Xyr1-binding site 5'-GGC(T/A)$_3$-3' (blue), Cre1-binding site 5'-SYGGRG-3' (orange), CCAAT-box (yellow), and TATA-box (black). Positions are indicated by the scale on top. Regions for CHART-PCR and *in vivo* footprinting analyses are marked by black bars and were termed CHART region 1 and 2, or footprint region 1 and 2, respectively.

In the case of *xyn1*, the CHART region 1 comprises a URR that was proven to be functional, whereas the CHART region 2 bears the TATA-box and putative transcription factor-binding sites in close proximity. The *cis* elements in the URR of *xyn1*, which were previously identified as functional *in vivo,* are a CCAAT-box (position -428), two Xyr1-binding sites (positions -404 and -420), and a double Cre1-binding site (positions -383 and -391) (Rauscher et al. 2006). In the case of *xyn2*, the CHART region 1 contains putative *cis* elements located further upstream. The CHART region 2 is located near the TATA-box and bears a previously described regulatory element of *xyn2*. The following *cis* elements belong to this region: a CCAAT-box (position -216) that is surrounded by two Xyr1-binding sites (positions -208 and -222), and one Cre1-binding site (position -188) (Würleitner et al. 2003, Stricker et al. 2008b).

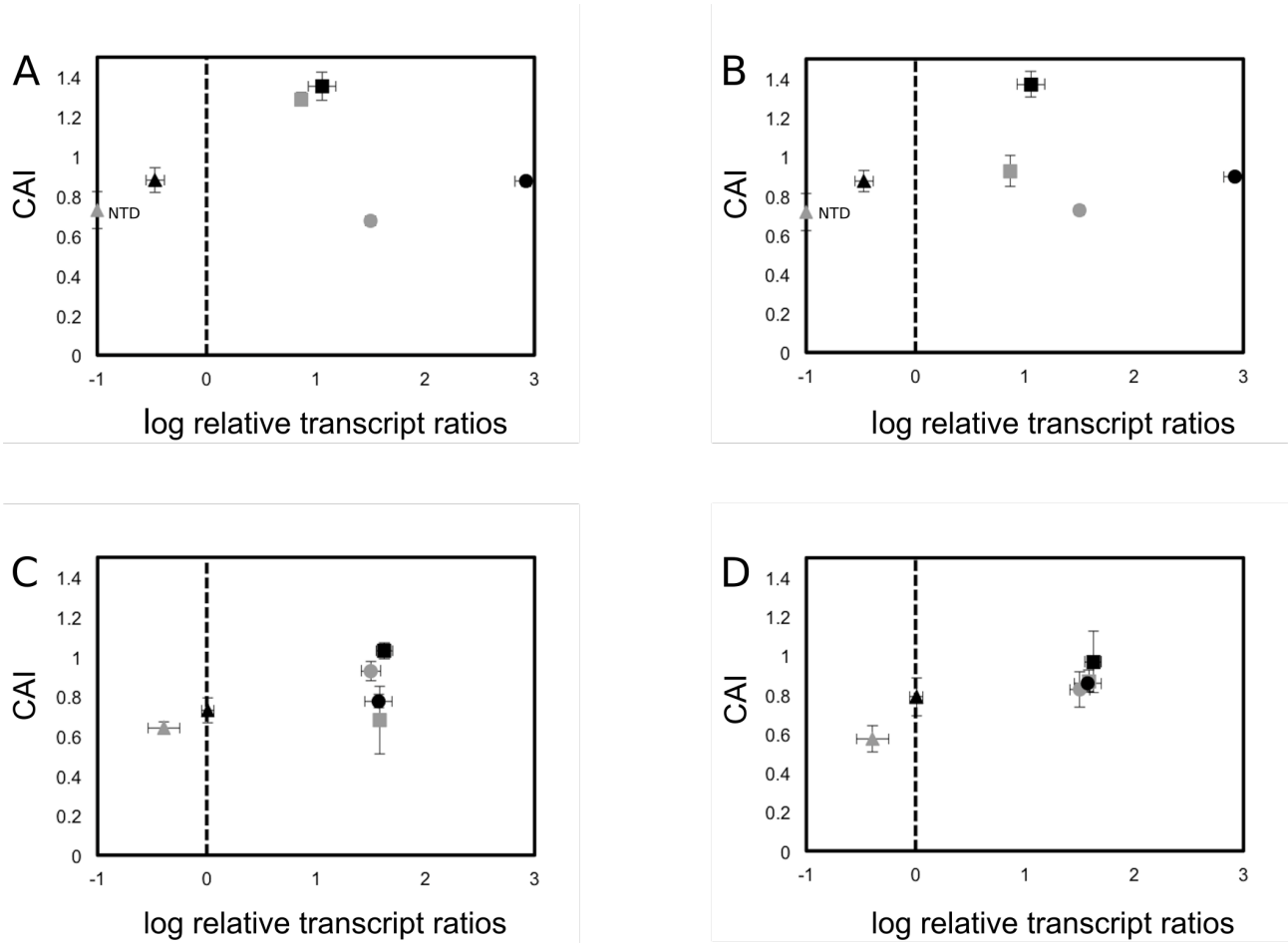

Fig 2 A-D – The chromatin status and the transcript levels were assessed by CHART-PCR analyses and RT-qPCR in the wild-type strain QM6a (grey) and in Rut-C30 (black). Both strains were pre-grown on glycerol and incubated for 3 h on D-glucose (triangles), D-xylose (circles), sophorose (squares), and no carbon source, which was used as the reference condition for transcript analysis (indicated by the dashed vertical lines). The relative transcript ratios are displayed in logarithmic scale on the x-axis and the chromatin accessibility indices (CAIs) are depicted on the y-axis. The transcript levels and the CAIs are normalized to *act* and *sar1*. NTD means "no transcript detected" and was set to -1. The results for the investigated CHART regions 1 (A, C) and 2 (B, D) are provided for *xyn1* (A, B) and *xyn2* (C, D).

In the case of *xyn1*, the chromatin status does not change on D-xylose in comparison to D-glucose in both CHART regions and strains (Fig. 2 A and B), but the transcript levels are considerably induced by D-xylose in both strains (Fig. 2 A or B). In Rut-C30, the extent of induction by D-xylose is even higher than in QM6a. The chromatin is slightly more open in Rut-C30 than in QM6a, which is a general trend also on the other investigated carbon sources (Fig. 2 A and B). The chromatin reacts differently on sophorose compared to D-xylose. A chromatin opening can be observed in the presence of sophorose compared to D-glucose for both strains and regions (Fig. 2 A and B). However, the extent of induction on sophorose was lower than on D-xylose in both strains. Altogether, an opening of chromatin did accompany the induction achieved with sophorose, but no opening was associated with an even more pronounced induction by D-xylose (Fig. 2 A and B).

In contrast to *xyn1*, an opening effect of the chromatin is observed on D-xylose compared to D-glucose in both investigated CHART regions of *xyn2* in QM6a (Fig. 2 C and D). Although, this opening did not occur in Rut-C30, *xyn2* gene expression is induced in both strains on D-xylose. The chromatin opening on D-xylose together with an increased transcript level was found in QM6a only (Fig. 2 C and D). Sophorose induces *xyn2* expression to a similar extent as D-xylose in both strains (Fig. 2 C and D). In the case of sophorose, the chromatin becomes more accessible compared to D-glucose in one of the investigated regions in each strain (CHART region 2 in QM6a, CHART region 1 in Rut-C30). Summarizing, the achieved induction (regardless of the inducing compound) was accompanied by an opening of chromatin in the wild-type strain, and a sophorose-specific opening in Rut-C30.

D-xylose changes protein-DNA interaction in the wild-type strain, but hardly in Rut-C30

In the course of transcription analyses, the expression of both xylanases was found to be induced by D-xylose in both strains (Fig. 2 A-D). However, the expression of *xyn1* can be induced stronger in Rut-C30 than in QM6a (Fig. 2 A and B). Interestingly, an opening of the chromatin didn't accompany the induction of *xyn1* expression by D-xylose in either strain, whereas it did for the induction of *xyn2* expression (Fig. 2 C and D). To study the strain-specific differences during induction of xylanase expression in detail, *in vivo* footprinting analyses were performed. Therefore, both strains were pre-grown on glycerol and transferred to D-glucose and D-xylose. A DMS treatment allowed us to capture *in vivo* DNA occupancy by proteins within two footprinting regions that were chosen based on the frequency of occurrence of transcription factor-binding sites and regulatory elements (Fig. 1).

We could detect strong differences of the protein-DNA interactions comparing D-xylose to D-glucose in the wild-type strain in the region 1 of the *xyn1* URR (-869 to -598) (Fig. 3 A). In Rut-C30, though, the differences in DNA occupancy between the two carbon sources were not as pronounced as in QM6a (Fig. 3 A). In comparison to region 1, the region 2 of the *xyn1* URR (positions -513 to -361) shows a different *in vivo* footprinting pattern. Less pronounced differences (concerning intensity and frequency) in protein-DNA interactions on D-xylose compared to D-glucose were detected in both strains (Fig. 3 B). In QM6a, the differences in protein-DNA interactions were mainly found on essential *cis* acting elements. In Rut-C30, the differences of DNA occupancies between D-xylose and D-glucose were detected in close proximity to one Xyr1-binding site (position -426) and to the Cre1-binding sites (-383, -391 and -466) (Fig. 3 B).

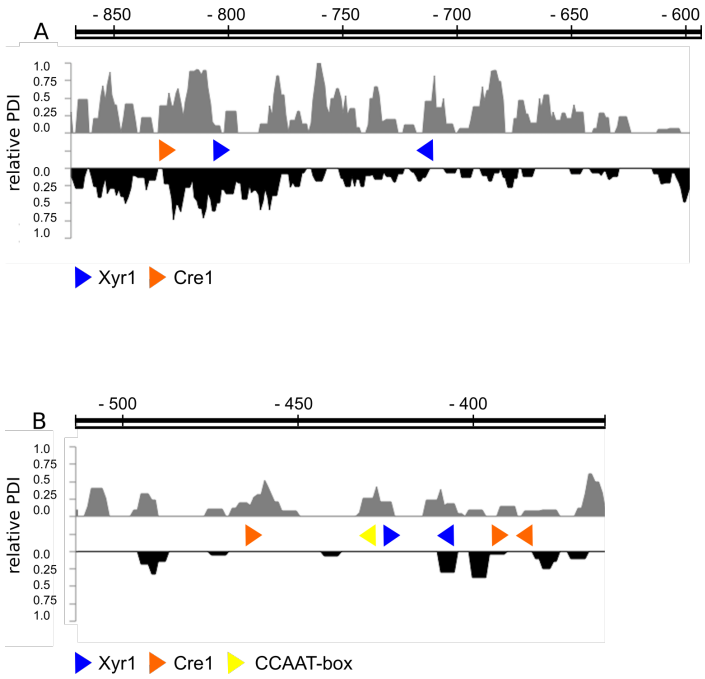

Fig. 3 A-B – *In vivo* footprinting landscapes of the *xyn1* URR are presented for footprinting regions 1 (A) and 2 (B). Fungal mycelia were pre-grown and transferred to D-xylose (inducing) and D-glucose (repressing). The chromosomal DNA was methylated *in vivo* by DMS. The profiles of the relative protein-DNA interaction indices (PDIs) of the wild-type strain QM6a (grey) and Rut-C30 (black) are depicted on the y-axis. The PDIs indicate differences in protein-DNA interactions on D-xylose compared to D-glucose for each strain and region. Putative transcription factor-binding sites within the URR (x-axis) are symbolized by coloured triangles: Xyr1 (blue), Cre1 (orange), and CCAAT-box (yellow). Positions are indicated by the scale on top.

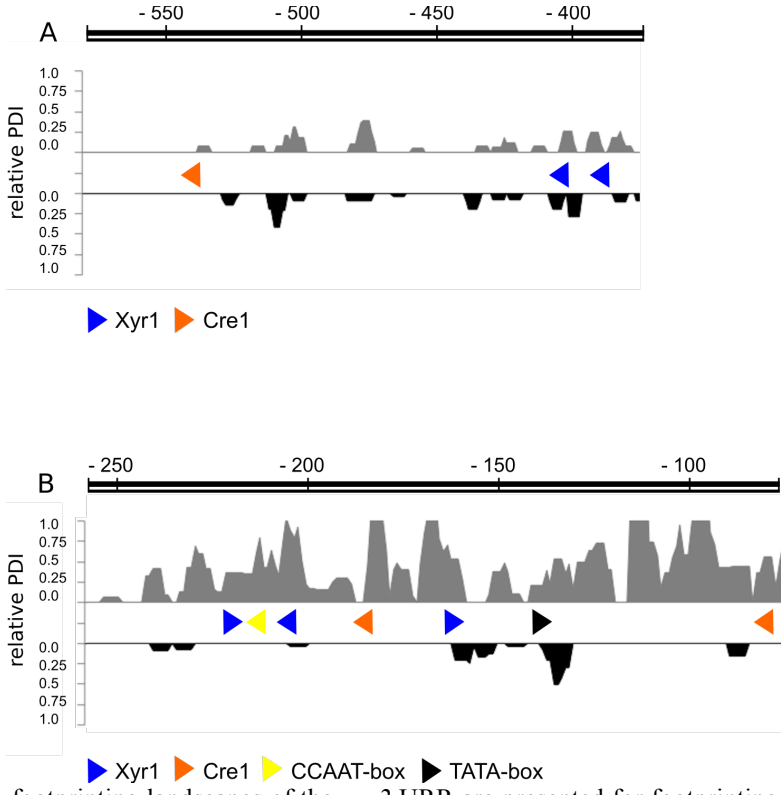

Fig 4 A-B – *In vivo* footprinting landscapes of the *xyn2* URR are presented for footprinting regions 1 (A) and 2 (B). Fungal mycelia were pre-grown and transferred to D-xylose (inducing) and D-glucose (repressing). The chromosomal DNA was methylated *in vivo* by DMS. The profiles of the relative protein-DNA interaction indices (PDIs) of the wild-type strain QM6a (grey) and Rut-C30 (black) are depicted on the y-axis. The PDIs indicate differences in protein-DNA interactions on D-xylose compared to D-glucose for each strain and region. Putative transcription factor-binding sites within the URR (x-axis) are symbolized by coloured triangles: Xyr1 (blue), Cre1 (orange), the CCAAT-box (yellow), and the TATA-box (black). Positions are indicated by the scale on top.

In the case of *xyn2*, we obtained for region 1 (positions -580 to -373) a similar pattern for both strains, *i.e.* we detected only a few changes in protein-DNA interactions on D-xylose compared to D-glucose (Fig. 4 A). However, in region 2 (positions -258 to -73) strong and frequently occurring differences in protein-DNA interactions between D-xylose and D-glucose were detected in the case of QM6a (Fig. 4 B). In contrast, the *in vivo* footprinting pattern in Rut-C30 shows again hardly any differences in DNA occupancy on D-xylose compared to D-glucose. Notably, the detected differences were found on and in close proximity to the TATA-box (Fig. 4 B).

Summarizing, for QM6a we found that in both genes (*i.e. xyn1* and *xyn2*) at least one region exhibits pronounced differences in protein-DNA interaction in response to D-xylose compared to D-glucose. In contrary, in Rut-C30, the DNA occupancy hardly changed in the presence of D-xylose compared to D-glucose. It is important to note that Rut-C30 had a slightly more open chromatin than QM6a and a better induction of *xyn1* expression triggered by D-xylose (compare Fig. 2 A and B). Considering all these observations, we hypothesize that the transcription machinery can access the generally more open chromatin in Rut-C30 more easily, resulting in a higher inducibility of the gene expression. However, neither the open chromatin status, nor the induction seems to be influenced by regulatory proteins binding specifically in response to the presence of D-xylose or D-glucose in Rut-C30 according to the *in vivo* footprinting analyses. A possible explanation for the lack of differences in the protein-DNA interaction between D-xylose and D-glucose might be the presence of a truncated version of Cre1, *i.e.* Cre1-96 (Mello-de-Sousa et al. 2014). It was reported that Cre1-96 is involved in the open chromatin status of the promoter regions of the cellulase-encoding genes *cbh1* and *cbh2*. Functional Cre1-sites were found to be occupied in these URRs under both, inducing and repressing conditions. Therefore, Mello-de-Sousa and co-workers suggested that Cre1-96 no longer binds DNA in a D-glucose-specific manner (Mello-de-Sousa et al. 2014). Consequently, we assume that Cre1-96 also binds on the investigated *xyn1* and *xyn2* URRs under both conditions, thereby contributing to the reduced differences observed in the *in vivo* footprinting analyses. Further, we suggest that the carbohydrate-independent binding of Cre1-96 is related to the more open chromatin in Rut-C30 detected under all conditions tested. However, this model does not explain the strong differences in induction between D-xylose and D-glucose of the *xyn1* and *xyn2* gene expression in Rut-C30. In this regard, the *in vivo* footprinting analyses point towards the TATA-box. The detected differences of DNA occupancies directly at the TATA-box in Rut-C30 suggest a hot spot of D-xylose-dependent interactions there, such as the assembly of the transcription machinery and/or recruiting proteins.

Protein-DNA interaction pattern is similar in the wild-type strain and Rut-C30 when applying the inducer sophorose

In the case of *xyn2*, a similar intensity of induction was achieved by sophorose as by D-xylose (Fig. 2 C or D). Therefore, we became interested in studying protein-DNA interactions on the *xyn2* URR under sophorose-induced conditions in an analogous experiment as performed for D-xylose. We conducted an *in vivo* footprinting analysis of mycelia samples incubated on sophorose and compared them to samples derived from incubation on D-glucose.

The *in vivo* footprinting analysis of region 1 resulted in rather small and regularly distributed differences comparing sophorose and D-glucose (Fig. 5 A). A clear *cis* element-specific pattern could not be observed for either strain, similarly to the results for the comparison of D-xylose to D-glucose (compare Fig. 5 A to Fig. 4 A).

As mentioned, strong differences in protein-DNA interactions were found across the region 2 on D-xylose compared to D-glucose in QM6a (Fig. 4 B). Using sophorose as an inducing substance, only minor differences in protein-DNA interactions were detected

compared to D-glucose, and even a complete loss of any interaction differences directly at the TATA-box was observed (Fig. 5 B). The Xyr1-binding sites remained occupied using sophorose as inducer in the wild-type strain, however, the differences to D-glucose were not as strong as on D-xylose (compare Fig. 5 B to Fig. 4 B). Interestingly, in Rut-C30, the *in vivo* footprinting pattern resulting from comparison of both inducers to D-glucose showed hardly any differences (compare Figs. 4 and 5 B). However, also in Rut-C30 a reduction in the intensity was found around the TATA-box when sophorose was used as inducer (Fig. 5 B) instead of D-xylose (Fig. 4 B).

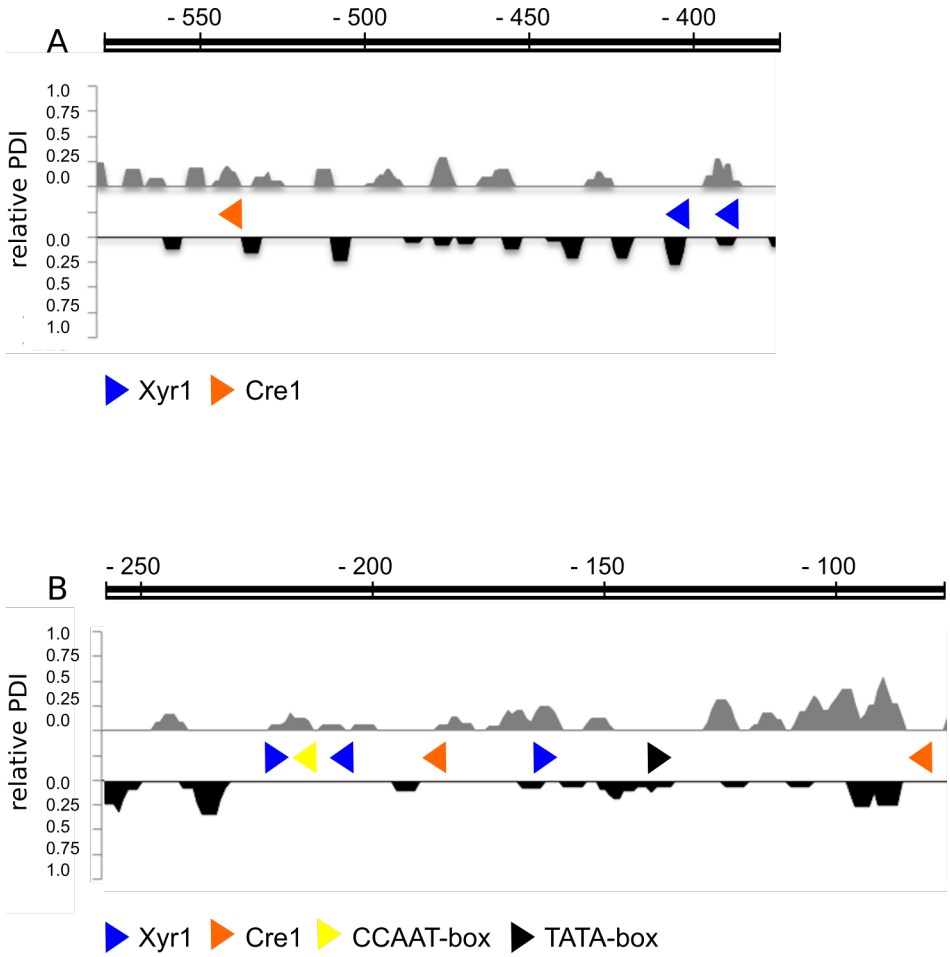

Fig 5 A-B – *In vivo* footprinting landscapes of the *xyn2* URR are presented for footprinting regions 1 (A) and 2 (B). Fungal mycelia were pre-grown and transferred to sophorose (inducing) and D-glucose (repressing). The chromosomal DNA was methylated *in vivo* by DMS. The profiles of the relative protein-DNA interaction indices (PDIs) of the wild-type strain QM6a (grey) and Rut-C30 (black) are depicted on the y-axis. The PDIs indicate differences in protein-DNA interactions on sophorose compared to D-glucose for each strain and region. Putative transcription factor-binding sites within the URR (x-axis) are symbolized by coloured triangles: Xyr1 (blue), Cre1 (orange), the CCAAT-box (yellow), and the TATA-box (black). Positions are indicated by the scale on top.

Altogether, it became apparent that the interplay of proteins contacting the DNA leads to a different pattern of *xyn2* expression (Würleitner et al. 2003, Stricker et al. 2008b). In the wild-type strain we generally observed different patterns for the two inducers, sophorose and D-xylose. In both strains the differences on the TATA-box were found to be less pronounced

on sophorose. In other words, the comparative *in vivo* footprinting patterns for sophorose for the wild-type strain became similar to those obtained for Rut-C30. For Rut-C30, it has previously been suggested that the *xyn2* URR is permanently bound by regulatory proteins and remains free of nucleosomes (Würleitner et al. 2003).

According to our results, sophorose – other than D-xylose – leads to a similar DNA occupancy as D-glucose in both strains. Bearing in mind that i) the chromatin became as loose on sophorose as on D-xylose (compared to D-glucose), and ii) that the extent of the achieved *xyn2* induction was also similar with both substances (Fig. 2 C and D), we speculated that induction by sophorose is mediated without additional proteins binding. There are possible alternative mechanisms, which would fit to the similar *in vivo* footprinting pattern, *e.g.*: i) regulatory proteins that act in a carbohydrate-specific manner bind somewhere else in the respective URR, ii) chromatin remodelers that act in a carbohydrate-specific manner bind equally distributed on the URR (yielding the observed, regular pattern of small differences), iii) chromatin remodelers or histone modifying proteins bind in a carbohydrate-unspecific manner, but differ in their action (*e.g.* histone acetyltransferases bind and provoke an opening of chromatin under inducing conditions, while under repressing conditions histone methyltransferases bind and provoke a more close chromatin).

However, all these hypotheses would mean that the type of signal transmission in case of D-xylose and sophorose is strikingly different. Regarding sophorose, a cAMP-dependent signal transmission was shown to be involved in enzyme production in *T. reesei* (Šesták & Farkaš 1992, Nogueira et al. 2015). Nogueria and co-workers found that the intracellular cAMP levels correlate directly with a higher induction level of cellulolytic enzyme expression in a sophorose-dependent manner (Nogueira et al. 2015). However, there does not exist such a study for the induction of xylanases in the presence of D-xylose or sophorose. Despite that, for *Aspergillus phoeniciis* and *Aspergillus sydowii* it was demonstrated that CCR of xylanase expression in the presence of D-glucose is similar as for *xyn1* in *T. reesei*. The repression in *Aspergillus* could be reverted by the addition of exogenous cAMP (Gosh & Nanda 1994, Rizzatti et al. 2008). Nonetheless the addition of exogenous cAMP did not revert the repression of cellulases on D-glucose in *T. reesei* (Šesták & Farkaš 1992), one could speculate that there might be a cAMP-dependent release of CCR in the case of xylanases in *T. reesei*.

for sophorose and D-xylose on the investigated region 2. Notably, this region bears the *cis* acting elements that were earlier described as functional for the regulation

Acknowledgements

This work was financed by two grants from the Austrian Science Fund (FWF): V232-B20 and P24851 given to Astrid R. Mach-Aigner, and by a doctoral program of TU Wien ("CatMat").

References

Aro N, Ilmén M, Saloheimo A, Penttilä M. 2003 – ACEI of *Trichoderma reesei* is a repressor of cellulase and xylanase expression. Applied and environmental Microbiology 69, 56–65.

Aro N, Saloheimo A, Ilmén M, Penttilä M. 2001 – ACEII, a novel transcriptional activator involved in regulation of cellulase and xylanase genes of *Trichoderma reesei*. The Journal of biological chemistry 276, 24309–24314.

Derntl C, Gudynaite-Savitch L, Calixte S, White T, Mach RL, Mach-Aigner AR. 2013 – Mutation of the Xylanase regulator 1 causes a glucose blind hydrolase expressing phenotype in industrially used *Trichoderma* strains. Biotechnology for biofuels 6, 62.

Derntl C, Rassinger A, Srebotnik E, Mach RL, Mach-Aigner AR. 2015 – Xpp1 regulates expression of xylanases but not of cellulases in *Trichoderma reesei*. Biotechnology for biofuels 8, 11.

Furukawa T, Shida Y, Kitagami N, Mori K, Kato M, Kobayashi T, Okada H, Ogasawara W, Morikawa Y. 2009 – Identification of specific binding sites for XYR1, a transcriptional activator of cellulolytic and xylanolytic genes in *Trichoderma reesei*. Fungal Genetics and Biology 46, 564–574.

Gorsche R, Jovanovic B, Gudynaite-Savitch L, Mach RL, Mach-Aigner AR. 2013 – A highly sensitive *in vivo* footprinting technique for condition-dependent identification of *cis* elements Nucleic Acids Research 42, e1.

Gosh M, Nanda G. 1994 – Physiological studies on xylose induction and glucose repression of xylanolytic enzymes in *Aspergillus sydowii* MG49. FEBS Microbiology Letters 117, 151–156.

Kuhls K, Leichfeldt E, Samules G, Kovacs W, Meyer W, Petrini O, Gams W, Börner T, Kubicek C. 1996 – Molecular evidence that the asexual industrial fungus *Trichoderma reesei* is a clonal derivative of the ascomycete *Hypocrea jecorina*. Proceedings of the National Academy of Science of the United States of America 93, 7755–7760.

Mach RL, Strauss J, Zeilinger S, Schindler M, Kubicek CP. 1996 – Carbon catabolite repression of xylanase I (*xyn1*) gene expression in *Trichoderma reesei*. Molecular Microbiology 21, 1273–1281.

Mach-Aigner AR, Grosstessner-Hain K, Pocas-Fonseca MJ, Mechtler K, Mach RL. 2010 – From an electrophoretic mobility shift assay to isolated transcription factors: a fast genomic-proteomic approach. BMC Genomics 11, 644.

Mandels M. 1985 – Applications of cellulases. Biochemical Society Transactions 13, 414–416.

Mello-de-Sousa TM, Gorsche R, Rassinger A, Pocas-Fonseca MJ, Mach RL, Mach-Aigner AR. 2014 – A truncated form of the Carbon catabolite repressor 1 increases cellulase production in *Trichoderma reesei*. Biotechnololy for Biofuels 7, 129.

Mello-de-Sousa TM, Rassinger A, Derntl C, Poças-Fonseca MJ, Mach-Aigner AR, Mach RL. 2016 – The Relation between chromatin status, Xyr1 and cellulase expression in *Trichoderma reesei*. Current Genomics 17, 1–8.

Mello-de-Sousa TM, Rassinger A, Pucher ME, dos Santos Castro L, Persinoti GF, Silva-Rocha R, Poças-Fonseca MJ, Mach RL, Silva RN, Mach-Aigner AR. 2015 – The impact of chromatin remodelling on cellulase expression in *Trichoderma reesei*. BMC Genomics 16.

Montenecourt BS, Eveleigh DE. 1979a – Production and characteriation of high yielding cellulase mutants of *Trichoderma reesei*. TAPPI Journal 28, 101–108.

Montenecourt BS, Eveleigh DE. 1979b. Selective Screening Methods for the Isolation of High Yielding Cellulase Mutants of *Trichoderma reesei*. In: Brown RD, Jurasek L, editors. Hydrolysis of Cellulose: Mechanisms of Enzymatic and Acid Catalysis. Washington, DC: American Chemical Society, 289–301.

Nogueira KMV, do Nascimento Costa M, de Paula RG, Mendonça-Natividade FC, Ricci-Azevedo R, Nascimento Silva. 2015 – Evidence of cAMP involvement in cellobiohydrolase expression and secretion by *Trichoderma reesei* in presence of the inducer sophorose. BMC Microbiology 15, 12.

Rauscher R, Würleitner E, Wacenovsky C, Aro N, Stricker AR, Zeilinger S, Kubicek CP, Penttilä M, Mach RL. 2006 – Transcriptional regulation of *xyn1*, encoding xylanase I, in *Hypocrea jecorina*. Eukaryotic Cell 5, 447–456.

Ries L, Belshaw NJ, Ilmén M, Penttilä ME, Alapuranen M, Archer DB. 2014 – The role of CRE1 in nucleosome positioning within the *cbh1* promoter and coding regions of *Trichoderma reesei*. Applied Microbiology and Biotechnology 98, 749–762.

Rizzatti ACS, Freitas FZ, Bertolini MC, Peixoto-Nogueira SC, Terenzi HF, Jorge JA, Polizeli MLTM. 2008 – Regulation of xylanase in *Aspergillus phoenicis*: a physiological and molecular approach. Journal of Industrial Microbiology and Biotechnology 35, 237–244.

Šesták S, Farkaš V. 1992 – Metabolic regulation of endoglucanase synthesis in *Trichoderma reesei*: participation of cyclic AMP and glucose-6-phosphate. Canadian Journal of Microbiology 39, 342–347.

Steiger MG, Mach RL, Mach-Aigner AR. 2010 – An accurate normalization strategy for RT-qPCR in *Hypocrea jecorina* (*Trichoderma reesei*). Journal of Biotechnology 145, 30–37.

Strauss J, Mach RL, Zeilinger S, Hartler G, Stoffler G, Wolschek M, Kubicek CP. 1995 – Cre1, the carbon catabolite repressor protein from *Trichoderma reesei*. FEBS Letters 376, 103–107.

Stricker AR, Grosstessner-Hain K, Würleitner E, Mach RL. 2006 – Xyr1 (xylanase regulator 1) regulates both the hydrolytic enzyme system and D-xylose metabolism in *Hypocrea jecorina*. Eukaryotic Cell 5, 2128–2137.

Stricker AR, Mach RL, de Graaff LH. 2008a – Regulation of transcription of cellulases- and hemicellulases-encoding genes in *Aspergillus niger* and *Hypocrea jecorina* (*Trichoderma reesei*). Applied Microbiology and Biotechnology 78, 211–220.

Stricker AR, Trefflinger P, Aro N, Penttilä M, Mach RL. 2008b – Role of Ace2 (Activator of Cellulases 2) within the *xyn2* transcriptosome of *Hypocrea jecorina*. Fungal Genetics and Biology 45, 436–445.

Teeri T, Salovouri, I., Knowles, J. 1983 – The molecular cloning of the major cellulase gene from *Trichoderma reesei*. Biotechnology 1, 696–699.

Törrönen A, Mach RL, Messner R, Gonzalez R, Kalkkinen N, Harkki A, Kubicek CP. 1992 – The two major xylanases from *Trichoderma reesei*: characterization of both enzymes and genes. Biotechnology (N Y) 10, 1461–1465.

Viikari L, Kantelinen A, Sundquist J, Linko M. 1994 – Xylanases in bleaching - from an idea to the industry. FEMS Microbiology Reviews 13, 335–350.

Würleitner E, Pera L, Wacenovsky C, Cziferszky A, Zeilinger S, Kubicek CP, Mach RL. 2003 – Transcriptional regulation of *xyn2* in *Hypocrea jecorina*. Eukaryotic Cell 2, 150–158.

Zeilinger S, Mach RL, Schindler M, Herzog P, Kubicek CP. 1996 – Different inducibility of expression of the two xylanase genes *xyn1* and *xyn2* in *Trichoderma reesei*. Journal of Biological Chemistry 271, 25624–25629.

Zeilinger S, Schmoll M, Pail M, Mach RL, Kubicek CP. 2003 – Nucleosome transactions on the *Hypocrea jecorina* (*Trichoderma reesei*) cellulase promoter *cbh2* associated with cellulase induction. Molecular Genetics and Genomics 270, 46–55.

Chapter 2

Peer-reviewed publication: ‚The Relation Between Promoter Chromatin Status, Xyr1 and Cellulase Expression in *Trichoderma reesei'* published in Current Genomics 17, 145-152 (2016)

Authors' Contributions

The author of this thesis, Alice Rassinger, performed the *in vivo* footprinting assays and participated in the conception of the *in vivo* footprinting data visualization.

Send Orders for Reprints to reprints@benthamscience.ae

Current Genomics, 2016, *17*, 145-152

The Relation Between Promoter Chromatin Status, Xyr1 and Cellulase Expression in *Trichoderma reesei*

Thiago M Mello-de-Sousa[1,†], Alice Rassinger[1,†], Christian Derntl[1], Marcio J. Poças-Fonseca[2], Robert L Mach[1] and Astrid R Mach-Aigner[1,*]

[1]*Department for Biotechnology and Microbiology, TU Wien, Vienna, Austria;* [2]*Department of Genetics and Morphology, Institute of Biological Sciences, University of Brasilia, Brasília-DF, Brazil*

A.R. Mach-Aigner

Abstract: The ascomycete *Trichoderma reesei* is used for the production of plant cell wall-degrading enzymes in industrial scale. The interplay of the transactivator Xyr1 and the repressor Cre1 mainly regulates the expression of these enzymes. During inducing conditions, such as in the presence of sophorose, the transcription of the two major cellulase-encoding genes, *cbh1* and *cbh2*, is activated as well as the expression of *xyr1*. In the presence of D-glucose carbon catabolite repression mediated by Cre1 takes place and the expression of Xyr1 and the plant cell wall-degrading enzymes is down-regulated. In this study we compare the chromatin status of *xyr1*, *cbh1*, and *cbh2* promoters in the wild-type strain and the Cre1-deficient strain Rut-C30. Chromatin rearrangement occurs in the *xyr1* promoter during induction on sophorose. Chromatin opening and protein-DNA interactions in the *xyr1* promoter were detected especially in a region located 0.9 kb upstream the translation start codon, which bears several putative Cre1-binding sites and a CCAAT-box. Moreover, the *xyr1* promoter is overall more accessible in a *cre1*-truncated background, no matter which carbon source is present. This makes the *xyr1* regulatory sequence a good target for promoter engineering aiming at the enhancement of cellulase production.

Keywords: Cellulases, Chromatin, Promoter, *Trichoderma reesei*, Rut-C30, Xyr1.

1. INTRODUCTION

The saprophytic ascomycete *Trichoderma reesei* (teleomorph *Hypocrea jecorina* [1]) is an industrially relevant microorganism due to its high capacity to secrete plant cell wall-degrading enzymes (PCWDE). These enzymes are applied in the food and textile, pulp and paper industry, and are a bottleneck for the cost-efficient production of second-generation biofuels. Details on applications of *T. reesei* enzymes are reviewed in [2, 3].

The expression of the PCWDE-encoding genes in *T. reesei* is controlled in large part by two transcriptions factors, *i.e.* the main transactivator Xyr1 and the mediator of carbon catabolite repression (CCR), Cre1. Xyr1 is a Zn_2Cys_6 binuclear cluster protein essential for expression of both, xylanases and cellulases [4]. It normally binds to 5'-$GGC(A/T)_3$-3'-motifs [5] arranged as inverted repeats in the promoters regions of its target genes. On most carbon sources *xyr1* is expressed at low levels, however, this can be induced by the disaccharide sophorose [6]. Within the Xyr1 regulon, the induction of the genes coding for the main cellulases (*i.e. cbh1* and *cbh2*) is directly associated with the extent of induction of *xyr1* expression, which is not observed for the other target genes of Xyr1 [6].

Cre1 is a C_2H_2-type zinc finger protein that binds to the consensus sequence 5′-SYGGRG-3′ [7]. In the presence of D-glucose, Cre1 mediates CCR in a double-lock mechanism by directly repressing the expression of some PCWDE-encoding genes [8, 9], and also the expression of *xyr1* itself [10]. It should be noted that the deletion of *cre1* in order to circumvent CCR is not a useful strategy. This deletion causes strong pleiotropic effects, *i.e.* a *cre1* deletion strain is strongly reduced in growth and therefore not convenient for industrial applications.

However, a strain suitable for industrial applications was derived from the *T. reesei* wild-type isolate QM6a by three rounds of mutagenesis. This strain, Rut-C30, was selected for high cellulase production and turned out to be released from Cre1-mediated CCR [11-13]. In total, Rut-C30 lacks over 100 kb of genomic DNA compared to the wild-type strain. In detail, it bears 15 small insertions, 223 point mutations, and 18 deletions [14, 15]. For example, an 83 kb large region containing 29 genes is missing in Rut-C30 [16, 17]. An important feature of Rut-C30 is the presence of a truncated form of the Carbon catabolite repressor 1 (Cre1-96, [7]). Cre1-96 contains only one of the two zinc finger motifs [18], however, it is still able to bind DNA [19]. This truncation does not only result in release from CCR, but additionally has a positive regulatory influence on the expression of target genes [19]. Notably, most industrially used strains originate from Rut-C30 [6, 14].

*Address correspondence to this author at the Department for Biotechnology and Microbiology, Institute of Chemical Engineering, TU Wien, Gumpendorfer Str. 1a, A-1060 Wien, Austria; Tel: +43 1 58801 166558; Fax: +43 1 5880117299;
E-mail: astrid.mach-aigner@tuwien.ac.at

†*Equal contributors.*

1875-5488/16 $58.00+.00

Despite the intense efforts to investigate the molecular mechanism underlying the regulation of cellulase production in *T. reesei* (reviewed in [20]), the mechanism of activation of gene expression is still not fully understood. Especially, information about the activation of expression of the *xyr1* gene is scarce. The same is true for possible additional levels of gene regulation within the Xyr1 regulon, such as chromatin remodeling. The upstream regulatory regions (URR) of the cellulase-encoding genes *cbh1* and *cbh2* have been previously subjects in studies focusing on nucleosome positioning and chromatin remodeling in response to different carbon sources. Former reports pointed towards Cre1 as an important factor in influencing chromatin packaging during repressing conditions [19, 21, 22]. During this study we investigated the chromatin accessibility status of the *xyr1, cbh1,* and *cbh2* promoter under repressing and inducing conditions. We aimed to learn more about the *xyr1* promoter architecture and the impact on the cellulase expression in a comparative study including Rut-C30 and the wild-type strain.

2. MATERIALS AND METHODS

2.1. Fungal Strains

The following *T. reesei* strains were used throughout this study: the wild-type strain QM6a (ATCC 13631) and the carbon catabolite derepressed strain Rut-C30 (ATCC 56765). Both strains were maintained on malt extract agar.

2.2. Growth Conditions

For carbon source replacement experiments mycelia were pre-cultured in 1-l Erlenmeyer flasks on a rotary shaker (180 rpm) at 30 °C for 24 h in 250 ml of Mandels-Andreotti (MA) medium [23] supplemented with 1 % (w/v) glycerol as sole carbon source. A total of 10^9 conidia per litre (final concentration) were used as inoculum. Pre-grown mycelia were washed and equal amounts were resuspended in 20 ml MA media containing 1 % (w/v) D-glucose or 2 mM sophorose or no carbon source, respectively, and were incubated for 3 h. Samples were derived from three biological replicates and were pooled before RNA extraction and chromatin digestion.

2.3. Analysis of Transcript Levels

Fungal mycelia were homogenized in 1 ml of peqGOLDTriFast DNA/RNA/protein purification system reagent (PEQLAB Biotechnologie, Erlangen, Germany) using a FastPrep(R)-24 cell disrupter (MP Biomedicals, Santa Ana, CA, USA). RNA was isolated according to the manufacturer's instructions, and the concentration was measured using the NanoDrop 1000 (Thermo Scientific, Waltham, US). Synthesis of cDNA from mRNA was carried out using the RevertAid™ H Minus First Strand cDNA Synthesis Kit (Thermo Scientific, Waltham, USA) according to the manufacturer's instructions. Quantitative, reverse transcription PCRs (RT-qPCRs) were performed in a Rotor-Gene Q system (Qiagen, Hilden, Germany). All reactions were performed in triplicates. The reaction mixture (final volume 15 µl) contained 7.5 µl 2 x iQ SYBR Green Mix (Bio-Rad, Hercules, USA), 100 nM forward and reverse primer and 2.5 µl cDNA (diluted 1:20). Primer sequences are provided in (Table **1**). Cycling conditions and control reactions were performed as described previously [24]. Data normalization using *sar1* and *act* as reference genes and calculations were performed as published previously [24].

2.4. Chromatin Accessibility Real-time PCR (CHART-PCR)

DNase I digestion of chromatin and quantitative PCR (qPCR) analysis were carried out as described before [19]. qPCR analysis of the DNase I-treated samples was performed to measure the relative abundance of target regions. PCRs were performed in triplicates in a Rotor-Gene Q system (Qiagen) using the reaction mixture (final volume 20 µl) and cycling conditions described before [19]. Primer sequences are provided in (Table **1**). The amount of intact input DNA of each sample was calculated by comparing the threshold values of the PCR amplification plots with a standard curve generated for each primer set using serial dilutions of genomic, undigested DNA. The chromatin accessibility index (CAI) was defined as: CAI = (Dc1+Dc2)/2Ds, where Ds is the amount of intact DNA detected for each target region and Dc1 and Dc2 are the amounts of intact DNA detected for the promoter regions of *sar1* and *act* respectively, used as reference genes for normalization.

2.5. *In Vivo* Footprinting Analysis

In vivo methylation using dimethyl sulphate (DMS) followed by ligation-mediated PCR was performed as described previously [25]. Primer sequences are provided in (Table **1**). The separation of fragments was performed by capillary gel electrophoresis (Microsynth, Balgach, Switzerland) and results were analyzed using the ivFAST program [25]. For the generation of the landscape visualization, the data sets of the coding and non-coding strand were combined, for each base pair the mean of the output value of this base pair and of the four adjacent base pairs was calculated, obtained mean values were converted to logarithmic scale, and given as the protein-DNA interaction index (PDI). In the case of no difference between compared conditions, termed 'n/a' in the ivFAST data output file, the value was set to 0.

3. RESULTS

3.1. Higher *xyr1* Expression Corresponds to Higher Chromatin Accessibility in the *xyr1* Promoter

We were interested to what extent chromatin accessibility of the *xyr1* promoter is linked to the transcript levels of *xyr1*. Therefore, we subjected the wild-type strain QM6a and Rut-C30 to a carbon source replacement experiment. After pregrowing both strains in MA medium containing glycerol, the obtained mycelia were transferred to MA medium containing sophorose (inducing condition), D-glucose (repressing condition) or no carbon source (reference condition) and were incubated for 3 h. First, CHART-PCR was employed to investigate the chromatin packaging of two *xyr1* promoter regions: the core promoter (position -216 to +35) bearing the TATA-box, and a putative URR (position -1038 to -742) bearing five Cre1-binding sites (positions -872, -878, -945, -963, and -972) and a CCAAT-box (-995, [26]) (Fig. **1A**). Complementary, the expression of *xyr1* was investigated by RT-qPCR in order to evaluate its relation to chromatin accessibility. The expression of *xyr1* is equally induced on sophorose in the two strains, whereas D-glucose represses

Table 1. Oligonucleotides used throughout this study.

Name	Sequence (5' -3')	Usage
Actfw	TGAGAGCGGTGGTATCCACG	RT-qPCR
Actrev	GGTACCACCAGACATGACAATGTTG	RT-qPCR
sar1fw	TGGATCGTCAACTGGTTCTACGA	RT-qPCR
sar1rev	GCATGTGTAGCAACGTGGTCTTT	RT-qPCR
cbh1f	GATGATGACTACGCCAACATGCTG	RT-qPCR
cbh1r	ACGGCACCGGGTGTGG	RT-qPCR
cbh2f	CTATGCCGGACAGTTTGTGGTG	RT-qPCR
cbh2r	GTCAGGCTCAATAACCAGGAGG	RT-qPCR
xyr1f	CCCATTCGGCGGAGGATCAG	RT-qPCR
xyr1r	CGAATTCTATACAATGGGCACATGGG	RT-qPCR
epiactinTr_f	CTTCCCTCCTTTCCTCCCCCTCCAC	*act* CHART, region -226 to +24
epiactinTr_r	GCGACAGGTGCACGTACCCTCCATT	*act* CHART, region -226 to +24
episar1Tr_f	GTCAGGAAATGCCGCACAAGCAAGA	*sar1* CHART, region -490 to -224
episar1Tr_r	TGTGTTTTACCGCCTTGGCCTTTGG	*sar1* CHART, region -490 to -224
epixyr1_1Tr_f	CCTTTGGCCATCTACACAAGAGCAA	*xyr1* CHART, region -1038 to -742
epixyr1_1Tr_r	CGCAATTTTTATTGCTGTTCGCTTC	*xyr1* CHART, region -1038 to -742
epixyr1_2Tr_f	CCGACAGCAGCAGTAGTCAGGTTTT	*xyr1* CHART, region -216 to +35
epixyr1_2Tr_r	TAGGCAGAATAGCGACGGAGAGGAT	*xyr1* CHART, region -216 to +35
epicbh1_1Tr_f	AAGGGAAACCACCGATAGCAGTGTC	*cbh1* CHART, region -902 to -610
epicbh1_1Tr_r	TTTCACTTCACCGGAACAAACAAGC	*cbh1* CHART, region -902 to -610
epicbh1_2Tr_f	GGATCGAACACACTGCTGCCTTTAC	*cbh1* CHART, region -301 to -27
epicbh1_2Tr_r	GGTTTCTGTGCCTCAAAAGATGGTG	*cbh1* CHART, region -301 to -27
epicbh2_1Tr_f	CGGATCTAGGGCAGACTGGGCATTG	*cbh2* CHART, region -587 to -338
epicbh2_1Tr_r	GTGTAGTGTTGCGCTGCACCCTGAG	*cbh2* CHART, region -587 to -338
epicbh2_2Tr_f	TGCAGCGCAACACTACACGCAACAT	*cbh2* CHART, region -355 to -62
epicbh2_2Tr_r	TGCGCCTCATACAGGGTCACAGTCC	*cbh2* CHART, region -355 to -62
RG161	[6-FAM]AGGAGGAGCACGAACTGGACCGCAA	*xyr1* URR iv fp, fwd
RG162	[6-FAM]GACACGACCAGAGAGCTCCATCATGG	*xyr1* URR iv fp, rev
RG149	[6-FAM]CCTGCTCAGAGCTTGGCGCGATTTC	*xyr1* core region iv fp, fwd
RG150	[6-FAM]TCGGGGTAGGCAGAATAGCGACGGA	*xyr1* core region iv fp, rev

xyr1 expression only in the wild-type strain (Fig. **1B, C**). In both strains, the induced *xyr1* transcript formation on sophorose went along with a more open chromatin status compared to D-glucose. This could be found in the investigated URR (Fig. **1B**) and in the core promoter (Fig. **1C**). However, a comparison of the strains under the same condition (*i.e.* D-glucose repression or sophorose-mediated induction) revealed that the chromatin is in all cases more accessible in Rut-C30 (Fig. **1B, C**). This indicates a generally more accessible *xyr1* promoter in Rut-C30 than in the wild-type strain.

3.2. A Condition-specific Predisposition for DNA Occupancy in the URR of the *xyr1* Promoter is Lost in Rut-C30

The observed, strain-specific differences in chromatin compaction of the *xyr1* promoter prompted us to perform a detailed investigation of the DNA accessibility. To this end,

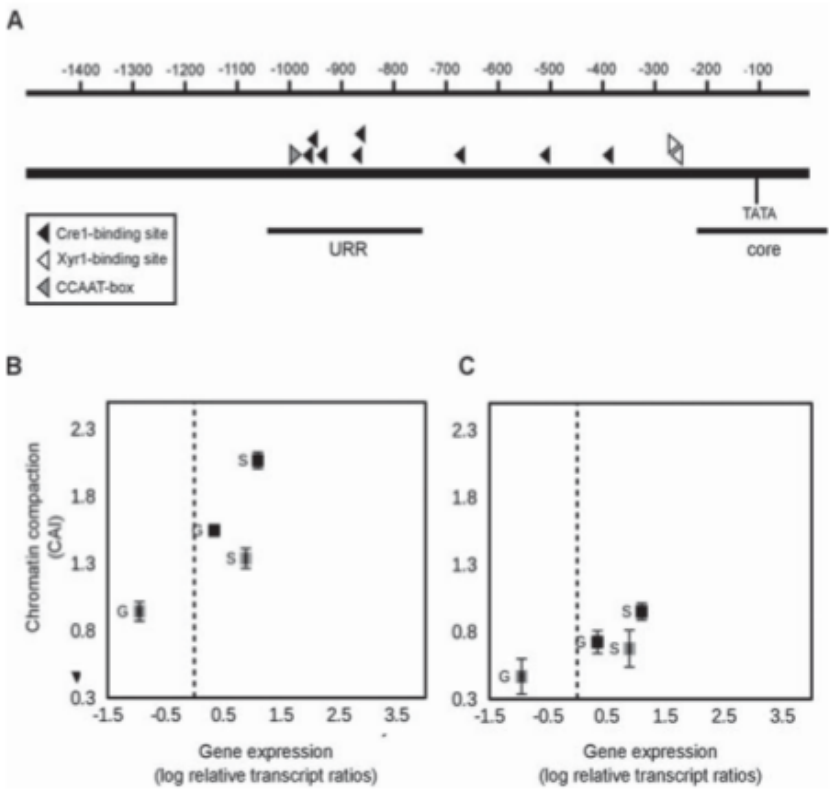

Fig. (1). Chromatin status and gene expression of *xyr1* in the wild-type strain and Rut-C30. (**A**) The promoter of *xyr1* is schematically represented. The scale at the top indicates the distance from the start codon in bp. Black bars indicate the positions of the core region (core) and the URR (URR) investigated by CHART-PCR. Triangles indicate *cis* elements. For CHART-PCR of the URR (**B**) and the core promoter (**C**) and *xyr1* transcript analysis (**B, C**) the *T. reesei* wild-type strain (grey squares) and Rut-C30 (black squares) were pre-grown on glycerol and thereafter incubated on D-glucose (G) or sophorose (S) for 3 h. CHART-PCR was performed by DNase I digestion followed by qPCR, and chromatin accessibility indices (CAIs) are depicted on the y-axis. The gene expression analysis was performed by cDNA synthesis followed by qPCR, and transcript levels are depicted on the x-axis. The dashed line indicates transcript level of the reference condition (wild-type strain, no carbon source, 3 h). *sar1* and *act* genes were used for data normalization. All values are means from measurements in triplicates and three biological replicates. Error bars indicate standard deviations. Diagrams are identically scaled.

in vivo footprinting analyses of an URR and the core promoter region were performed to identify differences in protein-DNA interaction patterns. Again, both strains were subjected to a carbon source replacement experiment as described above, followed by DMS-induced *in vivo* methylation. We could detect high DNA occupancy signals in the vicinity of the TATA-box, indicating a highly active transcription of *xyr1* in both strains during sophorose induction (Fig. **2B**). This is in good accordance with the before observed sophorose-mediated induction of transcript formation (compare Fig. **1B, C**). However, an overall analysis of the two regions resulted in different profiles for the two strains. Rut-C30 exhibited a repetitive signal appearance along the two analyzed regions, indicating widespread differences in DNA accessibility on sophorose and D-glucose (Fig. **2A, B**). In contrary, in the wild-type strain, the footprinting patterns turned out to differ between the two investigated *xyr1* promoter regions. For the URR we detected a high number of strong signals indicating considerable increased protein-DNA interaction under inducing condition compared to repressing condition (Fig. **2A**) while less and weaker signals were detected in the core promoter (Fig. **2B**). Altogether, these data support the assumption of a generally higher chromatin accessibility within the *xyr1* promoter in Rut-C30. It should be noted that we detected more and higher signals in the URR of QM6a than in the one of Rut-C30 (Fig. **2A**). The increased chromatin accessibility in the URR of the wild-type strain might be necessary to result in the same high transcript levels of *xyr1* during sophorose induction as in Rut-C30. Finally, we found that a single Xyr1-binding site (5'-GGCTAT-3', position -265 on the non-coding strand) is occupied in both strains, with stronger signals for Rut-C30 (Fig. **2C**). A second, non-canonical Xyr1-binding site (5'-GGGTTA-3', position – 270 on the coding strand) close to the first one was detected.

3.3. Expression of Cellulase-encoding Genes is Not Directly Influenced By the Promoter Chromatin Status During Early Induction

We observed a higher accessible chromatin status in the *xyr1* promoter in Rut-C30 compared to the wild-type strain. To examine whether this is also present in the targets genes of Xyr1, we comparatively investigated the chromatin status of the core promoter and an URR of the *cbh1* and *cbh2* genes each. Complementary, we analyzed their transcript levels. In contrast to what was observed for *xyr1*, no remarkable differences in the chromatin status of the *cbh1* (Fig. **3C, D**) nor

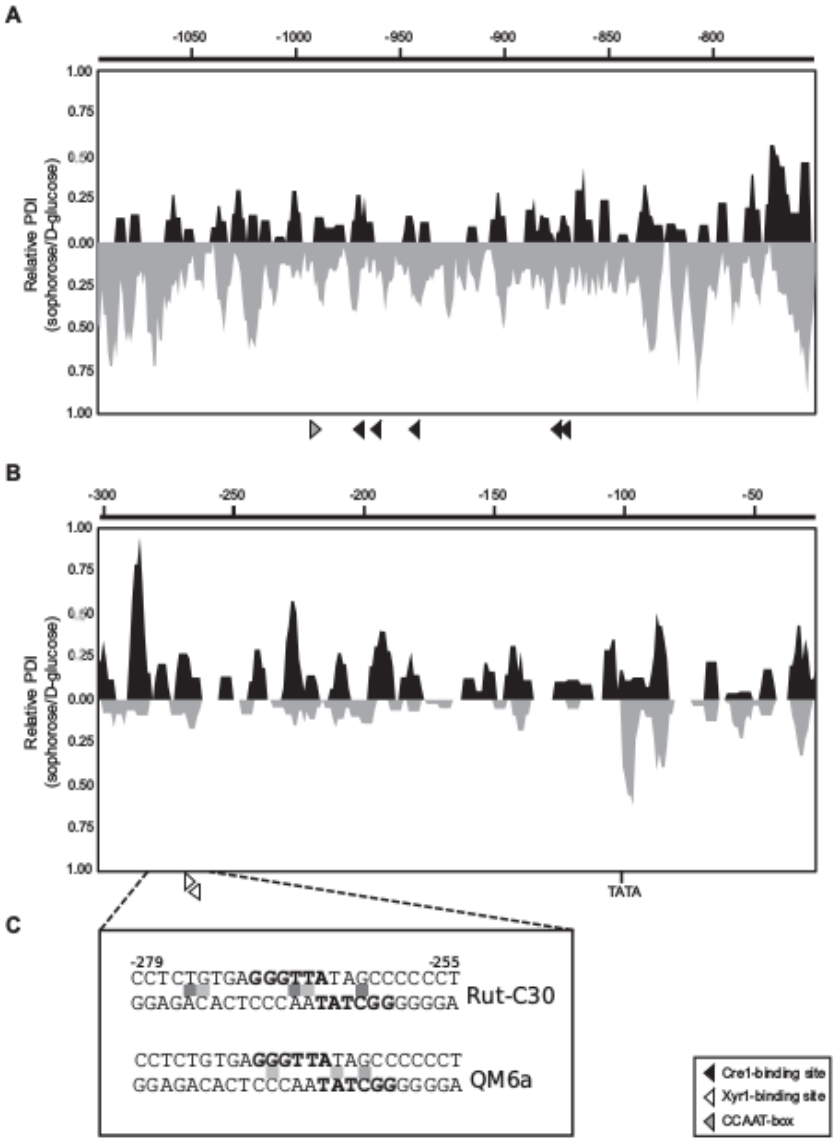

Fig. (2). *In vivo* foot printing analysis of the *xyr1* promoter. The *T. reesei* wild-type strain (grey landscape) and Rut-C30 (black landscape) were pre-grown on glycerol and then incubated on D-glucose or sophorose for 3 h followed by DMS-induced *in vivo* methylation. An URR (**A**) and the core promoter (**B**) were investigated. Triangles indicate *cis* elements. Analysis of data was performed using ivFAST [25] followed by a landscape-like visualization. The relative protein-DNA-interaction indices (PDI) give differences between the *in vivo* footprinting patterns obtained on sophorose compared to D-glucose of one strain. The diagrams are identically scaled and are comparable amongst the two strains within one region. The scale at the top indicates distance from the start codon in bp. (**C**) Detailed *in vivo* footprint result for both strains of the region -279 to -255 bearing two overlapping Xyr1-binding sites (bold letters). Methylation differences between sophorose and D-glucose are represented by light grey (1.1- to 1.3-fold) and dark grey squares (more than 1.3-fold).

of the *cbh2* (Fig. **3E, F**) promoters could be detected between the two strains. Besides this, we detected a slight sophorose-specific chromatin opening for each strain compared to D-glucose (Fig. **3C-F**). As expected, expression of both genes on D-glucose was partly released from CCR in Rut-C30. Transcript levels of *cbh1* and *cbh2* under inducing conditions were similar in both strains (Fig. **3C** and **E**), which fits to the before observed equal *xyr1* transcript levels (compare Fig. **1B**). Even if the above described results point to a relation between the chromatin status of the promoter and transcript formation in case of the *xyr1* gene, the expression of the *cbh1* and *cbh2* genes during early induction seem to be rather a consequence of the levels of Xyr1 than influenced by the chromatin status of their own promoters.

4. DISCUSSION

It has recently been reported that chromatin remodeling is associated with gene expression of PCWDEs in *T. reesei* in dependence of the carbon source used [19, 21, 22]. Moreover, Xyr1 is absolutely required for activation of PCWDE-encoding genes since a *xyr1* deletion fully abolishes their expression [4, 27]. However, up to now it remained completely unstudied whether chromatin remodeling is also influencing the expression of *xyr1* itself, and thereby,

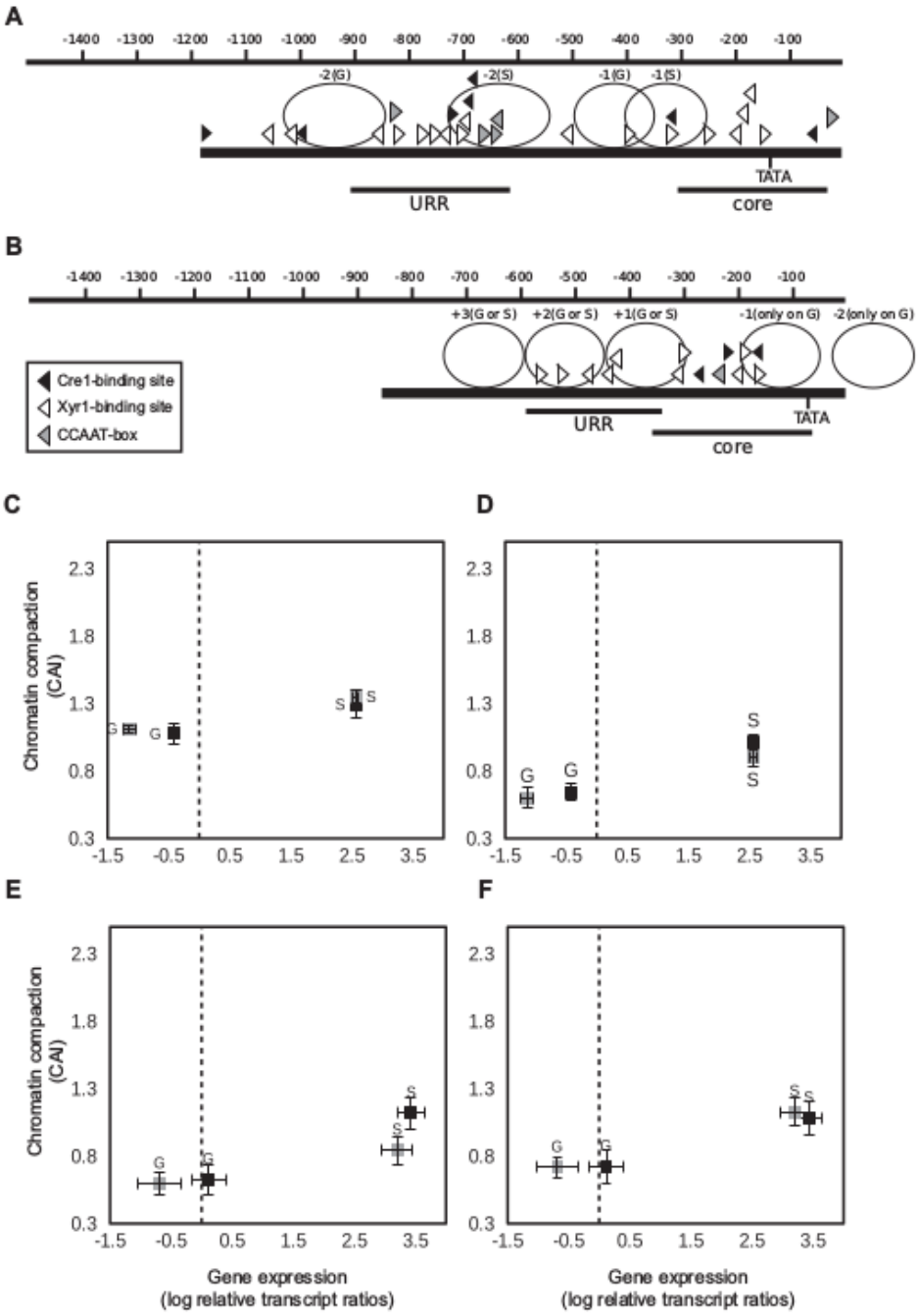

Fig. (3). Chromatin status and gene expression of cellulase-encoding genes in the wild-type strain and Rut-C30. The promoters of *cbh1* (**A**) and *cbh2* (**B**) are schematically represented. The scale at the top indicates the distance from the start codon in bp. Black bars indicate the positions of the core region (core) and the URR (URR) investigated by CHART-PCR. Triangles indicate *cis* elements. Carbon source-specifically positioned nucleosomes [21, 22] are indicated by ellipses. (**C-F**) The *T. reesei* wild-type strain (grey squares) and Rut-C30 (black squares) were pre-grown on glycerol and thereafter incubated on D-glucose (G) or sophorose (S) for 3 h. The URR (**C, E**) and the core promoter region (**D, F**) of the *cbh1* (**C, D**) and *cbh2* (**E, F**) genes were investigated each. CHART-PCR was performed by DNase I digestion followed by qPCR, and chromatin accessibility indices (CAIs) are depicted on the y-axis. The gene expression analysis was performed by cDNA synthesis followed by qPCR, and transcript levels are depicted on the x-axis. The dashed line indicates transcript level of the reference condition (wild-type strain, no carbon source, 3 h). *sar1* and *act* genes were used for data normalization. All values are means from measurements in triplicates and three biological replicates. Error bars indicate standard deviations. Diagrams are identically scaled.

might influence PCWDE-encoding gene expression in an indirect way. We found that induction-specific opening of chromatin is a lot more pronounced in the *xyr1* promoter than in those of the target genes, *cbh1* and *cbh2*. In the case of *xyr1* this chromatin opening goes hand in hand with higher gene expression, while for the target genes *cbh1* and *cbh2* the early induction is not directly related with opening of the chromatin. However, nucleosome positioning in *cbh1* and *cbh2* has previously been studied in *T. reesei* [21, 22]. Comparing the wild-type strain with *cre1*-deficient strains

(including Rut-C30) revealed that in the latter no positioned nucleosomes are present in the coding region of *cbh1* during cultivation on D-glucose. The authors also suggested a repositioning of promoter nucleosomes during inducing condition. Another study reported that two nucleosomes downstream of an *cbh2* activating element lose their positioning in a Cre1 positive background during induction, whereas Rut-C30 constitutively lacked strictly positioned nucleosomes on the *cbh2* promoter under all conditions tested [22]. Both studies emphasize a possible role of Cre1 in organizing the local chromatin structure in *cbh1* and *cbh2* during repressing conditions. It was speculated that a loss of functional Cre1 results in a less dense chromatin structure during CCR. At first glance, the similar chromatin compaction in the wild-type strain and Rut-C30 on D-glucose, which was observed during this study, seem to contradict these earlier studies. However, considering the time frame of the experiments, they turn out to be complementary. The previous nucleosome mapping in *cbh1* was investigated in a time course experiment by direct cultivation of the strains [21], and data for *cbh2* were obtained from longer incubation times after the carbon source replacement [22]. As we investigated the chromatin status already after 3 h, it is likely that chromatin remodeling had only influenced the transactivator-encoding gene expression. This led to enough available Xyr1 that consecutively positively influenced the expression of *cbh1* and *cbh2*. This conclusion is in accordance with the previously reported strict dependence of gene expression of *cbh1* and *cbh2* on the level of *xyr1* [6]. We suppose that the previously observed chromatin remodeling in the promoters of the target genes (*chb1* and *cbh2*) takes place during later cultivation stages. The authors would even suggest that Xyr1 then even contributes to a chromatin opening in the URR of cellulase-encoding genes since recently obtained data support this hypothesis (Mello-de-Sousa *et al.*, 2015, unpublished data).

Notably, we found that a *cre1* truncation background contributes to higher *xyr1* expression that goes along with chromatin opening regardless the condition employed. The increased accessibility of chromatin in Rut-C30 was verified by *in vivo* footprinting. During this experiment we detected a canonical Xyr1-binding site next to a non-canonical site in the *xyr1* promoter. It should be mentioned that previous *in vivo* footprinting analyses also detected active non-canonical Xyr1-binding sites (bearing up to two mismatches) in the *cbh2* and *xyn2* promoters [25]. The occuring Xyr1 double binding site (typically arranged as an inverted repeat) in the *xyr1* promoter points towards an eventual autoregulatory mechanism. According to the *in vivo* footprinting analysis this Xyr1-binding motif is stronger contacted Rut-C30. This would allow more available Xyr1 in Rut-C30, which might explain the observed differences between the strains on sophorose.

In the case of D-glucose the strongest differences in chromatin accessibility between Rut-C30 and wild-type strain were observed for the *xyr1* URR. This region bears five putative Cre1-binding sites and a CCAAT-box. The close position of the 5'-SYGGRG-3' motifs to each other and the strong signals detected in the wild-type strain point to an occupation by Cre1. This is a likely explanation for the more compact chromatin status observed in the wild-type strain on D-glucose. The presence of a CCAAT-box reinforces the importance of this region since the interaction of this *cis* element with the HAP2/3/5 complex is required for chromatin remodeling and full transcriptional activation of *cbh2* [22, 28]. *In vivo* footprinting analysis carried out in this study highlighted strong protein-DNA interactions in both strains at this motif during sophorose induction.

5. CONCLUSION

The investigation of chromatin accessibility of the *xyr1*, *cbh1,* and *cbh2* promoters revealed that during early induction chromatin rearrangement targets primary the *xyr1* promoter. An upstream regulatory region in the *xyr1* promoter was detected to be an important target of chromatin opening, probably involving regulation by Cre1 interaction and the protein complex HAP2/3/5. Consequently, the *xyr1* promoter represents a high potential target for strain engineering and employing approaches involving heterochromatin control of gene expression.

LIST OF ABBREVIATIONS

CAI	=	Chromatin accessibility index
CCR	=	Carbon catabolite repression
CHART-PCR	=	Chromatin accessibility real-time PCR
Cre1	=	Carbon catabolite repressor 1
DMS	=	Dimethyl sulphate
MA	=	Mandels Andreotti
PCWDEs	=	Plant cell wall-degrading enzymes
PDI	=	Protein-DNA interaction index
qPCR	=	Quantitative PCR
RT-qPCR	=	Quantitative, reverse transcription PCR
URR	=	Upstream regulatory region
Xyr1	=	Xylanase regulator 1

CONFLICT OF INTEREST

The author(s) confirm that this article content has no conflict of interest.

ACKNOWLEDGEMENTS

TMMS participated in conception of the study, performed CHART-PCR, transcript analyses, and drafted the manuscript. AR participated in conception of the landscape visualization of the *in vivo* footprinting data and carried out the footprinting analyses. CD participated in conception of the landscape visualization of the *in vivo* footprinting data and revision of the manuscript. RLM and MJPF participated in conception of the study and revision of the manuscript. ARMA participated in conception of the study, supervision of experiments, and revision of the manuscript. All authors read and approved the final manuscript. This work was supported by two grants from the Austrian Science Fund (FWF): V232-B20, P24851 given to ARMA, and by a doctoral program of Vienna University of Technology ("CatMat").

REFERENCES

[1] Kuhls, K.; Lieckfeldt, E.; Samuels, G.; Kovacs, W.; Meyer, W.; Petrini, O.; Gams, W.; Borner, T.; Kubicek, C. Molecular evidence that the asexual industrial fungus Trichoderma reesei is a clonal derivative of the ascomycete Hypocrea jecorina. *Proc. Natl. Acad. Sci. U S A*, **1996**. *93*, 7755 - 7760.

[2] Chundawat, S.P.; Beckham, G.T.; Himmel, M.E.; Dale, B.E. Deconstruction of lignocellulosic biomass to fuels and chemicals. *Annu. Rev. Chem. Biomol. Eng.*, **2011**. *2*, 121-145.

[3] Viikari, L.; Vehmaanperä, J.; Koivula, A. Lignocellulosic ethanol: From science to industry. *Biomass and Bioenergy*, **2012**. *46*(0), 13-24.

[4] Stricker, A.; Grosstessner-Hain, K.; Wurleitner, E.; Mach, R. Xyr1 (xylanase regulator 1) regulates both the hydrolytic enzyme system and D-xylose metabolism in Hypocrea jecorina. *Eukaryot. Cell.*, **2006**. *5*, 2128-2137.

[5] Furukawa, T.; Shida, Y.; Kitagami, N.; Mori, K.; Kato, M.; Kobayashi, T.; Okada, H.; Ogasawara, W.; Morikawa, Y. Identification of specific binding sites for XYR1, a transcriptional activator of cellulolytic and xylanolytic genes in Trichoderma reesei. *Fungal Genet. Biol.*, **2009**. *46*, 564 - 574.

[6] Derntl, C.; Gudynaite-Savitch, L.; Calixte, S.; White, T.; Mach, R.; Mach-Aigner, A. Mutation of the Xylanase regulator 1 causes a glucose blind hydrolase expressing phenotype in industrially used Trichoderma strains. *Biotechnol. Biofuels*, **2013**. *6*(1), 62.

[7] Strauss, J.; Mach, R.; Zeilinger, S.; Hartler, G.; Stoffler, G.; Wolschek, M.; Kubicek, C. Cre1, the carbon catabolite repressor protein from Trichoderma reesei. *FEBS Lett.*, **1995**. *376*, 103-107.

[8] Mach, R.; Strauss, J.; Zeilinger, S.; Schindler, M.; Kubicek, C. Carbon catabolite repression of xylanase I (xyn1) gene expression in Trichoderma reesei. *Mol. Microbiol.*, **1996**. *21*, 1273-1281.

[9] Ilmen, M.; Onnela, M.; Klemsdal, S.; Keranen, S.; Penttila, M. Functional analysis of the cellobiohydrolase I promoter of the filamentous fungus Trichoderma reesei. *Mol. Gen. Genet.*, **1998**. *257*, 386.

[10] Mach-Aigner, A.; Pucher, M.; Steiger, M.; Bauer, G.; Preis, S.; Mach, R. Transcriptional regulation of xyr1, encoding the main regulator of the xylanolytic and cellulolytic enzyme system in Hypocrea jecorina. *Appl. Environ. Microbiol.*, **2008**. *74*, 6554-6562.

[11] Montenecourt, B.; Eveleigh, D. Semiquantitative plate assay for determination of cellulase production by Trichoderma viride. *Appl. Environ. Microbiol.*, **1977**. *33*, 178-183.

[12] Montenecourt, B.; Eveleigh, D. Preparation of mutants of Trichoderma reesei with enhanced cellulase production. *Appl. Environ. Microbiol.*, **1977**. *34*, 777-782.

[13] Montenecourt, B.; Eveleigh, D. Selective Screening Methods for the Isolation of High Yielding Cellulase Mutants of Trichoderma reesei. in *Hydrolysis of cellulose: mechanisms of enzymatic and acid catalysis*; Brown, R; L, J; Eds.; American Chemical Society, **1979**; pp. 289-301.

[14] Peterson, R.; Nevalainen, H. Trichoderma reesei RUT-C30--thirty years of strain improvement. *Microbiology*, **2012**. *158*(Pt 1), 58-68.

[15] Le Crom, S.; Schackwitz, W.; Pennacchio, L.; Magnuson, J.; Culley, D.; Collett, J.; Martin, J.; Druzhinina, I.; Mathis, H.; Monot, F.; Seiboth, B.; Cherry, B.; Rey, M.; Berka, R.; Kubicek, C.; Baker, S.; Margeot, A. Tracking the roots of cellulase hyperproduction by the fungus Trichoderma reesei using massively parallel DNA sequencing. *Proc. Natl. Acad. Sci. USA*, **2009**. *106*, 16151-16156.

[16] Seidl, V.; Gamauf, C.; Druzhinina, I.; Seiboth, B.; Hartl, L.; Kubicek, C. The Hypocrea jecorina (Trichoderma reesei) hypercellulolytic mutant RUT C30 lacks a 85kb (29 gene-encoding) region of the wild-type genome. *BMC Genomics*, **2008**. *9*, 327.

[17] Vitikainen, M.; Arvas, M.; Pakula, T.; Oja, M.; Penttila, M.; Saloheimo, M. Array comparative genomic hybridization analysis of Trichoderma reesei strains with enhanced cellulase production properties. *BMC Genomics*, **2010**. *11*, 441.

[18] Ilmen, M.; Thrane, C.; Penttila, M. The glucose repressor gene cre1 of Trichoderma: isolation and expression of a full-length and a truncated mutant form. *Mol. Gen. Genet.*, **1996**. *251*, 451-460.

[19] Mello-de-Sousa, T.; Gorsche, R.; Rassinger, A.; Pocas-Fonseca, M.; Mach, R.; Mach-Aigner, A. A truncated form of the carbon catabolite repressor 1 increases cellulase production in Trichoderma reesei. *Biotechnol. Biofuels*, **2014**. *7*, 129.

[20] Stricker, A.; Mach, R.; de Graaff, L. Regulation of transcription of cellulases- and hemicellulases-encoding genes in Aspergillus niger and Hypocrea jecorina (Trichoderma reesei). *Appl. Microbiol. Biotechnol.*, **2008**. *78*, 211-220.

[21] Ries, L.; Belshaw, N.; Ilmen, M.; Penttila, M.; Alapuranen, M.; Archer, D. The role of CRE1 in nucleosome positioning within the cbh1 promoter and coding regions of Trichoderma reesei. *Appl. Microbiol. Biotechnol.*, **2014**. *98*, 749-762.

[22] Zeilinger, S.; Schmoll, M.; Pail, M.; Mach, R.; Kubicek, C. Nucleosome transactions on the Hypocrea jecorina (Trichoderma reesei) cellulase promoter cbh2 associated with cellulase induction. *Mol. Genet. Genomics*, **2003**. *270*, 46-55.

[23] Mandels, M. Applications of cellulases. *Biochem. Soc. Trans.*, **1985**. *13*, 414-416.

[24] Steiger, M.; Mach, R.; Mach-Aigner, A. An accurate normalization strategy for RT-qPCR in Hypocrea jecorina (Trichoderma reesei). *J. Biotechnol.*, **2010**. *145*, 30-37.

[25] Gorsche, R.; Jovanovic, B.; Gudynaite-Savitch, L.; Mach, R.; Mach-Aigner, A. A highly sensitive *in vivo* footprinting technique for condition-dependent identification of cis elements. *Nucleic Acids Res.*, **2014**. *42*, e1.

[26] Mantovani, R. A survey of 178 NF-Y binding CCAAT boxes. *Nucleic Acids Res.*, **1998**. *26*(5), 1135-1143.

[27] Stricker, A.; Steiger, M.; Mach, R. Xyr1 receives the lactose induction signal and regulates lactose metabolism in Hypocrea jecorina. *FEBS Lett*, **2007**. *581*, 3915 - 3920.

[28] Zeilinger, S.; Mach, R.; Kubicek, C. Two adjacent protein binding motifs in the cbh2 (cellobiohydrolase II- encoding) promoter of the fungus Hypocrea jecorina (Trichoderma reesei) cooperate in the induction by cellulose. *J. Biol. Chem.*, **1998**. *273*, 34463-34471.

Received: May 11, 2015 **Revised: May 19, 2015** **Accepted: June 10, 2015**

Chapter 3

Peer-reviewed publication: ‚A truncated form of the Carbon catabolite repressor 1 increases cellulase production in *Trichoderma reesei*' published in Biotechnology for Biofuels 7 (129) (2014)

Authors' Contributions

The author of this thesis, Alice Rassinger, performed the *in vivo* footprinting assays.

Biotechnology for Biofuels

RESEARCH ARTICLE Open Access

A truncated form of the Carbon catabolite repressor 1 increases cellulase production in *Trichoderma reesei*

Thiago M Mello-de-Sousa[1†], Rita Gorsche[1†], Alice Rassinger[1], Marcio J Poças-Fonseca[2], Robert L Mach[1] and Astrid R Mach-Aigner[1*]

Abstract

Background: Rut-C30 is a cellulase-hyperproducing *Trichoderma reesei* strain and, consequently, became the ancestor of most industry strains used in the production of plant cell wall-degrading enzymes, in particular cellulases. Due to three rounds of undirected mutagenesis its genetic background differs from the wild-type QM6a in many ways, of which two are the lack of a 83 kb large sequence in scaffold 15 and the partial lack of the gene encoding the Carbon catabolite repressor 1 (CREI). However, it is still unclear, what exactly enhances cellulase production in Rut-C30.

Results: The investigation of the expression of two genes encoding cellulases (*cbh1* and *cbh2*) and the gene encoding their main transactivator (*xyr1*) revealed that the presence of the truncated form of CREI (CREI-96) contributes more to the Rut-C30 phenotype than a general loss of CREI-mediated carbon catabolite repression (*cre1* deletion strain) or the deletion of 29 genes encoded in the scaffold 15 (83 kb deletion strain). We found that the remaining *cre1* in Rut-C30 (*cre1-96*) is transcribed into mRNA, that its putative gene product (Cre1-96) is still able to bind DNA, and that the CREI-binding sites in the upstream regulatory regions of the chosen CREI-target genes are still protected in Rut-C30. As it was previously reported that CREI acts on the nucleosome positioning, we also analyzed chromatin accessibility of the core promoters of CREI-target genes and found them open even on D-glucose in the presence of CREI-96.

Conclusions: The lack of the full version of CREI in Rut-C30 corresponds with a partial release from carbon catabolite repression but is not completely explained by the lack of CREI. In contrast, the truncated CREI-96 of Rut-C30 exerts a positive regulatory influence on the expression of target genes. Mechanistically this might be explained at least partially by a CREI-96-mediated opening of chromatin.

Keywords: *Trichoderma reesei*, *Hypocrea jecorina*, Rut-C30, Cellulases, Carbon catabolite repressor 1, Chromatin

Background

The filamentous ascomycete *Trichoderma reesei* is a saprophyte known for its ability to efficiently degrade biomass material by plant cell wall (PCW)-degrading enzymes. A genome-wide analysis identified 10 cellulolytic and 16 hemicellulolytic enzyme-encoding genes in *T. reesei* [1], of which the two most prominent cellulose-degrading enzymes are the cellobiohydrolases CBHI and CBHII (EC 3.2.1.91) [2]. However, the defining feature of this fungus is the exceedingly high amount of secreted enzymes that provoked its industrial exploitation for their production. Next to the pulp and paper industry [3], the food and feed industry [4], and the textile industry [5], these enzymes are applied in the production of biofuels [4]. With regards to cellulosic ethanol, the production costs of the needed enzymes massively influence the price and the competitiveness of the end-product. As a result their efficient expression remains an important topic of research.

The ancestor of most current industry strains is Rut-C30 [6,7]. It was derived from the *T. reesei* wild-type isolate QM6a through three rounds of mutagenesis (ultraviolet (UV) light and N-nitroguanidine) followed by a screening

* Correspondence: astrid.mach-aigner@tuwien.ac.at
†Equal contributors
[1]Department for Biotechnology and Microbiology, Institute of Chemical Engineering, Vienna University of Technology, Gumpendorfer Str. 1a, A-1060 Wien, Austria
Full list of author information is available at the end of the article

for the release from carbon catabolite repression (CCR) and high cellulase activity [8-10]. Since then the study of the specific physiological and genetic changes in Rut-C30 has been of interest [7,11] and a number of properties have been identified, for example, a 83 kb large region located in scaffold 15, which encodes 29 genes is lacking in Rut-C30 [12,13]. Another important property of Rut-C30 is the lack of the full version of the Carbon catabolite repressor 1 (CREI, [14]) having left a *cre1* sequence that would only encode for one of the two zinc finger regions of CREI (96 aa long) [15]. The native CREI is a C_2H_2-type zinc finger protein with the consensus sequence 5′-SYGGRG-3′ [14], and is orthologous to CreA from *Aspergillus* sp. [16-18] and MIG1 from *Saccharomyces cerevisiae* [19].

In *T. reesei* CREI is known to act on a number of regulatory levels. Firstly, it directly represses transcription of several genes encoding for PCW-degrading enzymes, for example the *cbh1* gene [20], by binding to tandem and inverted repeats in their upstream regulatory regions (URRs) [20,21]. Secondly, in the presence of D-glucose it represses the expression of the main transactivator of PCW-degrading enzyme expression, the Xylanase regulator 1 (XYRI) [22,23]. XYRI is a Gal4-like Zn2Cys6 binuclear cluster protein, of which the expression can be induced by sophorose [6] or as above-mentioned, repressed by D-glucose. Notably, the extent of induction of *xyr1* gene expression directly correlates with the induction of *cbh1* and *cbh2* gene expression, which is not the case for other genes in the XYRI regulon [6]. As a third regulatory level, CREI has been reported to play an essential role in correct nucleosome positioning, for example in the promoters of the *cbh1* and *cbh2* genes [24,25]. Altogether, CREI plays a major role in the regulation of 250 genes, both in a repressing and inducing way [26].

In this study we investigated to which extent the two mentioned striking genetic properties of Rut-C30, namely the lack of the 83 kb in scaffold 15 and the absence of a full CREI contribute to its cellulase hyper-producing phenotype. A special focus was studying the role of the remaining truncated version of CREI with regard to the transcriptional regulation of target gene expression, the ability of DNA binding, and the influence on the chromatin structure. The PCW-degrading enzyme-encoding genes *cbh1* and *cbh2*, as well as *xyr1* as the gene encoding their transactivator, were chosen as the CREI-target genes to be analyzed.

Results

The expression profile of *cbh1*, *cbh2*, and *xyr1* in QM6a-CREI$_{96}$ is closest to Rut-C30

In order to find out which genetic properties of Rut-C30 contribute to its cellulase hyper-producing phenotype we compared its expression profile to three transgenic strains. Two of them bear Rut-C30-related mutations, namely Δscaff15, which is a QM6a-derived strain with an 83 kb deletion in scaffold 15, and QM6a-CREI$_{96}$, which bears the truncated CREI version like Rut-C30 does. We also included a QM6a-derived *cre1* deletion strain because the phenotype of Rut-C30 is sometimes associated with the lack of CREI. We investigated expression levels of *cbh1*, *cbh2*, and *xyr1* under sophorose-inducing conditions. Interestingly, the transcript levels of all three genes were most similar in QM6a-CREI$_{96}$ compared to Rut-C30, while in the case of the other two strains (Δ*cre1* and Δscaff15) considerably lower levels were detected (Figure 1a, b, c). This result raised the consideration that regulatory molecular mechanisms are related to the truncated version of *cre1* remaining in the Rut-C30 genome.

CREI sites in upstream regulatory regions of target genes are strongly protected from DNA methylation in Rut-C30

All above-mentioned analyzed genes (*cbh1*, *cbh2*, and *xyr1*) are under the regulatory influence of CREI [20,22,25]. To learn if the protection patterns against DNA methylation of the URRs bearing CREI sites of these genes differ between the wild-type QM6a and Rut-C30, we performed *in vivo*/*in vitro* footprinting analyses. URRs of all three genes were investigated after both strains were pre-grown on glycerol and then incubated on D-glucose for 3 hours followed by dimethyl sulphate (DMS)-induced *in vivo* methylation. The footprinting pattern obtained for all genes showed the same or even stronger DNA occupancy in Rut-C30 compared to QM6a (Figure 2a, b, c). This finding prompted us to analyze if the truncated *cre1* (*cre1-96*) in Rut-C30 is transcribed. Thus, after pre-growth both strains were transferred to media containing D-glucose as a repressing condition, sophorose as an inducing condition, and no carbon source as a control condition respectively, and incubated for 3 hours. While we detected a low basal transcript level (originating from the native *cre1* gene) in the wild-type, we found increased levels in Rut-C30, whereupon the increase was more pronounced on D-glucose and sophorose than without carbon source (Figure 3a). Since the *cre1-96* mRNA could be detected in high amounts in Rut-C30 regardless of the applied condition (D-glucose or sophorose), we again performed *in vivo/in vitro* footprinting to investigate if the DNA protection pattern changes condition-dependent. We analyzed the same URRs of *cbh1*, *cbh2*, and *xyr1* genes comparing the application of D-glucose and sophorose. As can be inferred from Figure 3b, c, d no condition-specific differences could be detected even though strong DNA occupancy at the CREI sites was observed. This fits the expression results and suggests that CREI-96 may no longer act in a D-glucose specific manner.

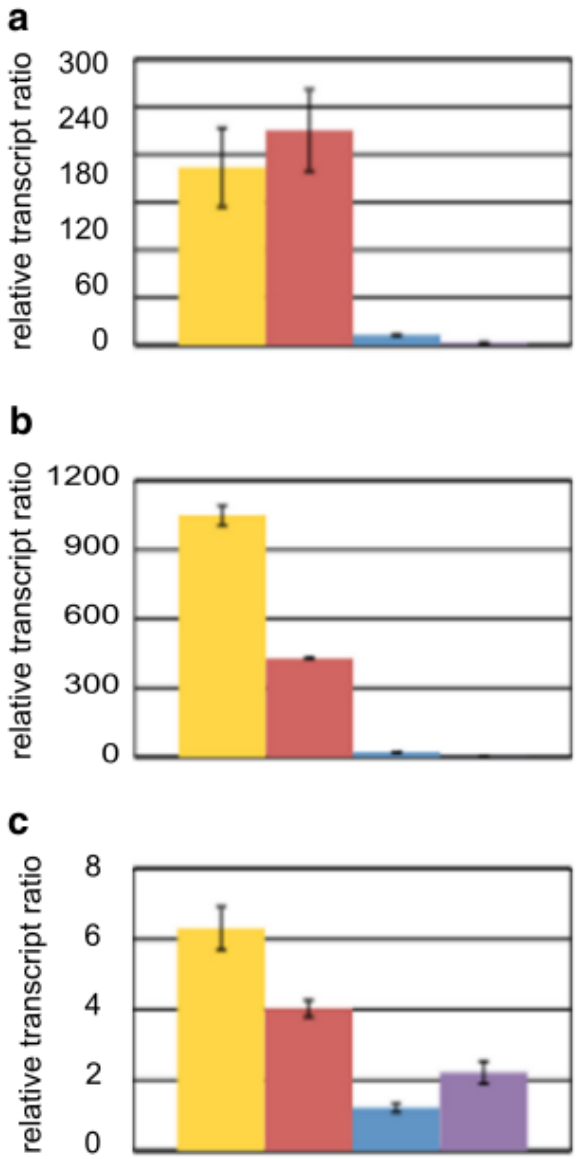

Figure 1 Transcript analysis in *Trichoderma reesei* strains bearing Rut-C30-related mutations. Rut-C30 (yellow bars), QM6a-CREI$_{96}$ (red bars), the Δ*cre1*-strain (blue bars), and the Δscaff15-strain (purple bars) were pre-grown on glycerol and then transferred to medium supplemented with sophorose and incubated for 3 hours. The transcript level analysis of the *cbh1* **(a)**, *cbh2* **(b)**, and *xyr1* **(c)** genes was performed by qPCR using *sar1* and *act* genes for data normalization. Levels refer to the wild-type strain QM6a incubated without carbon source. The values are means from measurements and biological experiments (cultivations) performed in triplicate. Error bars indicate standard deviations.

The truncated CREI-96 protein of Rut-C30 can bind to DNA *in vitro*

The results described above raise the question of whether the putative CREI-96 protein is still able to bind to DNA, especially because it lacks one of the two zinc fingers. To answer this question, we performed an electrophoretic mobility shift assay (EMSA) using the URR of *cbh1* covering three functional CREI-binding sites as a probe (Figure 4a). The applied CREI-96 protein was heterologously expressed as GST-fusion protein and thrombin-cleaved before usage. The assay yielded two bands (Figure 4b), which represent most likely the binding of one or more CREI-96 proteins to the sites of the probe. Similar results were observed before reporting that shorter versions of CREI can still bind target DNA sequences yielding more than one band [28]. However, both complexes are specifically formed because the bands were diminished by adding a cold competitor, while they remained unchanged by adding a specifically mutated competitor (Figure 4b). Altogether, this supports the working hypothesis that the truncated CREI-96, which is putatively formed in Rut-C30, is still able to bind its DNA target sequences. It should be noted that in filamentous fungi other regulatory proteins are known that are also able to bind their DNA with a single zinc finger, such as the *Aspergillus nidulans* AreA [29].

Higher gene expression corresponds with more open chromatin in QM6a-CREI$_{96}$

As we had strong indication that the truncated version of CREI-96 is present in Rut-C30 and still is able to bind the URRs of its target genes, we aimed to get more insights on its potential regulatory role. Consequently, QM6a-CREI$_{96}$ and the *cre1* deletion strain were grown on D-glucose and samples were drawn after 36, 39, 42, and 45 hours of cultivation. Because CREI was reported to be involved in nucleosome positioning within the *cbh1* and the *cbh2* promoter of *T. reesei* [24,25], we investigated the chromatin packaging by applying chromatin accessibility real-time PCR (CHART-PCR) analysis of the core promoter regions of the *cbh1*, *cbh2*, and *xyr1* genes. Second, we investigated the expression of these genes by RT-qPCR to see if there was a correlation of transcript levels with the chromatin accessibility. We could detect a higher expression of *cbh1* and *cbh2* genes in QM6a-CREI$_{96}$ compared to the Δ*cre1*-strain, which corresponded with a more open chromatin in the core promoters of the two genes in QM6a-CREI$_{96}$ (Figure 5a, b). The higher transcript levels of cellulase-encoding genes in QM6a-CREI$_{96}$ were reflected by increased enzyme activity (45.8 ± 1.5 U/mg dry weight;) measured after 45 hours of cultivation on D-glucose compared to the Δ*cre1*-strain (29.1 ± 1.8 U/mg dry weight). Interestingly, we found that in QM6a-CREI$_{96}$ the gene expression increased with a simultaneous opening of chromatin, in particular in *xyr1* and *cbh1* (Figure 5a). On the other hand, we could not observe a correlation of gene expression and chromatin accessibility in the *cre1* deletion strain (Figure 5b).

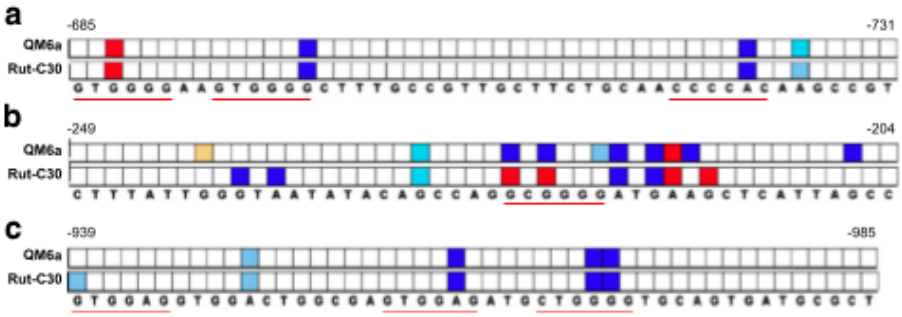

Figure 2 *In vivo* and *in vitro* footprinting analyses of URRs of CREI-target genes. The *Trichoderma reesei* wild-type strain QM6a and Rut-C30 were pre-grown on glycerol and then incubated on D-glucose for 3 hours followed by DMS-induced *in vivo* methylation. An URR bearing functional CREI sites (underlined in red) of the *cbh1* **(a)**, *cbh2* **(b)**, and *xyr1* **(c)** genes was investigated, and methylated, naked DNA was used as the reference. Numbers indicate the position of the base upstream from ATG. Analysis of data and visualization was performed using ivFAST (*in vivo* footprinting analysis software tool) [27]. Only signals that are statistically different are considered. Protected bases are highlighted in red shades and hypersensitive bases are highlighted in blue shades. The three colour intensities each correspond to stronger differences between compared conditions; increasing colour intensity means more than 1.4-, 1.6-, and 1.8-fold difference in *cbh1* and *cbh2* **(a, b)**, and more than 2.4-, 2.6-, and 2.8-fold difference in *xyr1* **(c)**.

To discover what this scenario looks like under inducing conditions, we applied the same experimental strategy on the two strains after pre-growth followed by incubation on sophorose for 30, 90, and 180 minutes. For *cbh1* and *cbh2* we observed in both strains an increase in transcript levels over time, which did not correlate in either of the two strains with a simultaneous opening of chromatin (Figure 6a, b). In the *xyr1* gene, transcript levels did not increase however, the chromatin became more compact over time (Figure 6a, b). Comparing the chromatin status of the two strains, the chromatin was slightly more accessible in QM6a-$CREI_{96}$ (Figure 6a, b).

CREI-96 upregulates the expression of a helicase-like transcription factor

Due to the results obtained from the CHART-PCR analyses, we assumed that the truncated CREI-96 was involved in chromatin remodelling in both a direct and indirect

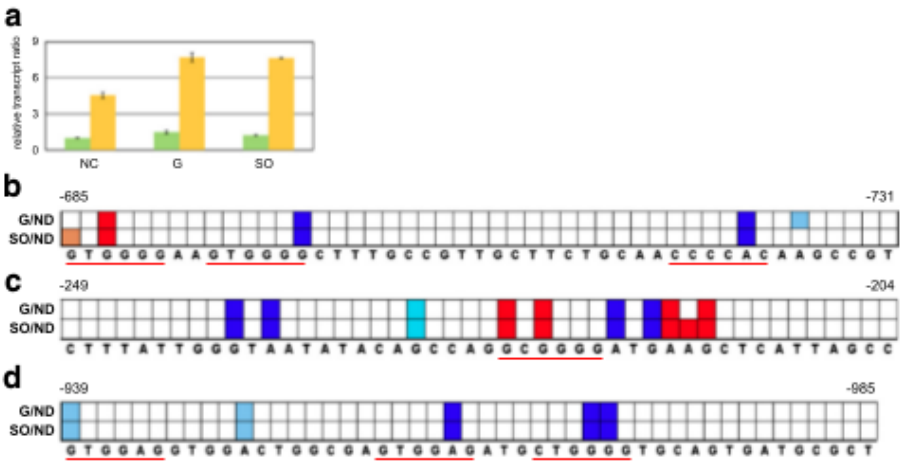

Figure 3 Analysis of the abundance of CREI-96 in Rut-C30. (a) The *Trichoderma reesei* wild-type strain QM6a (green bars) and Rut-C30 (yellow bars) were pre-grown on glycerol and then transferred to media supplemented with D-glucose (G), sophorose (SO) or without carbon source (NC), respectively, and incubated for 3 hours. The transcript level analysis of *cre1-96* was performed by qPCR using *sar1* and *act* genes for data normalization. Levels refer to the wild-type strain incubated without carbon source. The values are means from measurements in triplicates and three biological experiments (cultivations). Error bars indicate standard deviations. **(b-d)** *In vivo* and *in vitro* footprinting analysis of URRs of CREI-target genes in Rut-C30, which was pre-grown on glycerol and then incubated on D-glucose (G) or sophorose (SO) for 3 hours followed by DMS-induced *in vivo* methylation. An URR bearing functional CREI sites (underlined in red) of the *cbh1* **(b)**, *cbh2* **(c)**, and *xyr1* **(d)** genes each was investigated, and methylated, naked DNA (ND) was used as the reference. Numbers indicate the position of the base upstream from ATG. Analysis of data and visualization was performed using ivFAST [27]. Colour codes are the same as in Figure 2.

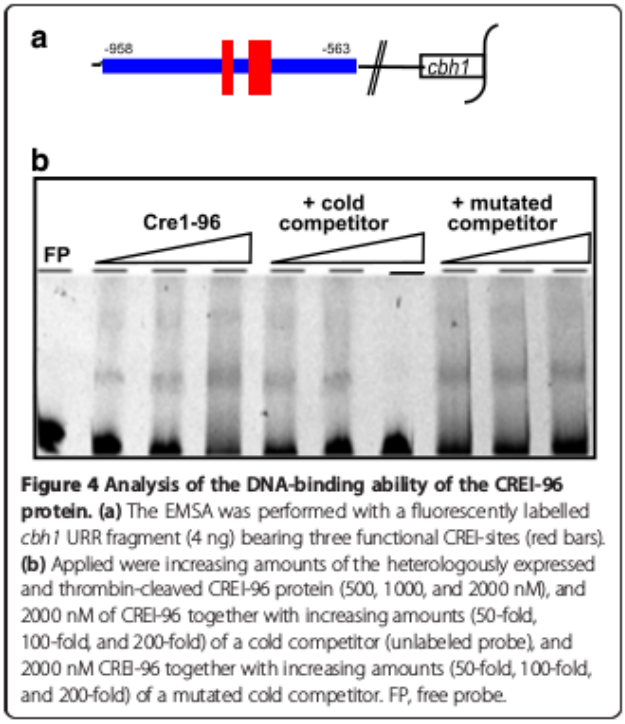

Figure 4 Analysis of the DNA-binding ability of the CREI-96 protein. (a) The EMSA was performed with a fluorescently labelled *cbh1* URR fragment (4 ng) bearing three functional CREI-sites (red bars). **(b)** Applied were increasing amounts of the heterologously expressed and thrombin-cleaved CREI-96 protein (500, 1000, and 2000 nM), and 2000 nM of CREI-96 together with increasing amounts (50-fold, 100-fold, and 200-fold) of a cold competitor (unlabeled probe), and 2000 nM CREI-96 together with increasing amounts (50-fold, 100-fold, and 200-fold) of a mutated cold competitor. FP, free probe.

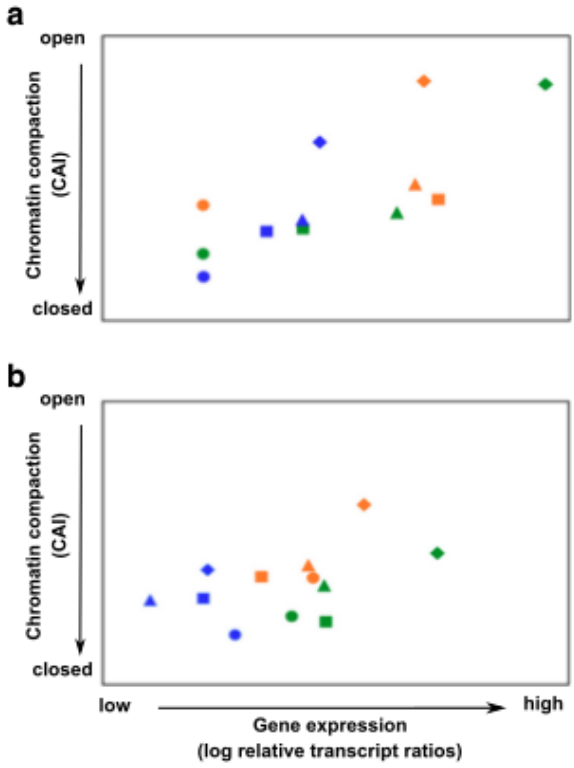

c

Gene	Spearman correlation	
	QM6a-CREI$_{96}$	QM6aΔ*cre1*
cbh1	0.94 (*P*<0.001)	0.47 (*P*=0.1161)
cbh2	0.35 (*P*=0.2714)	0.49 (*P*=0.0636)
xyr1	0.91 (*P*<0.001)	-0.38 (*P*=0.2705)

Figure 5 Transcript and CHART analysis of *Trichoderma reesei* CREI-mutant strains during growth on D-glucose. QM6a-CREI$_{96}$ **(a)** and the Δ*cre1*-strain **(b)** were grown on D-glucose and samples were taken after 36 (dots), 39 (boxes), 42 (triangles), 45 (diamonds) hours. The *cbh1* (green), *cbh2* (orange), and *xyr1* (blue) genes were investigated. The gene expression analysis was performed by cDNA synthesis followed by qPCR, and transcript levels (log) are depicted on the x-axis. CHART-PCR was performed by Dnase I digestion followed by qPCR, and CAIs are depicted on the y-axis. In both cases *sar1* and *act* genes were used for data normalization and QM6a-CREI$_{96}$ grown for 36 hours was the reference condition. All values are means from measurements in triplicates and three biological experiments (cultivations). Standard deviations were below 5%. Diagrams are identically scaled. **(c)** Spearman's rank correlation coefficients were calculated (close to −1 indicates negative correlation; close to 0 indicates no linear correlation; close to 1 indicates positive correlation). The *P*-values for each correlation coefficient were calculated to determine significance of data (how different from zero). $P > 0.05$ was considered as indicative of no linear correlation.

manner. Therefore, we searched the *T. reesei* genome for chromatin-remodelling proteins. We selected seven proteins, of which the annotation pointed to an involvement in chromatin rearrangement, for further investigation (Table 1). To determine a potential regulatory influence by CREI-96 we investigated their transcript levels in QM6a-CREI$_{96}$ and the Δ*cre1*-strain. Amongst the seven genes we observed one with different transcript levels, namely the gene encoding a helicase-like transcription factor (Protein ID 44747). Here we detected strong up-regulation in QM6a-CREI$_{96}$ compared to the Δ*cre1*-strain, regardless of whether the samples from the D-glucose growth experiment (Figure 7a) or the sophorose replacement (Figure 7b) were investigated. We term the aforementioned gene in this study *htf1* (helicase-like transcription factor 1). It should be noted that in previous reports this gene was called *snf2*, although it is not homologous to SNF2 of *Saccharomyces cerevisiae* [30]. However, the increased expression of *htf1* in QM6a-CREI$_{96}$ might be one reason for the observed change in chromatin.

Discussion

For a long time its lack of the full version of CREI has been considered to be a positive genetic property of Rut-C30 because it leads to a partial carbon catabolite de-repression. However, Rut-C30 still possesses a short version of CREI, CREI-96. During this study it became clear that this protein still has a function and influences the expression of target genes, notably, in a positive manner. We found three ways in which CREI-96 mechanistically exerts its role as a regulatory protein. Firstly, it acts directly on promoters of target genes. The short CREI-96 (lacking one zinc finger) can still bind to target DNA sequences *in vitro*, which leads *in vivo* to a clear protection pattern from DNA methylation at CREI-

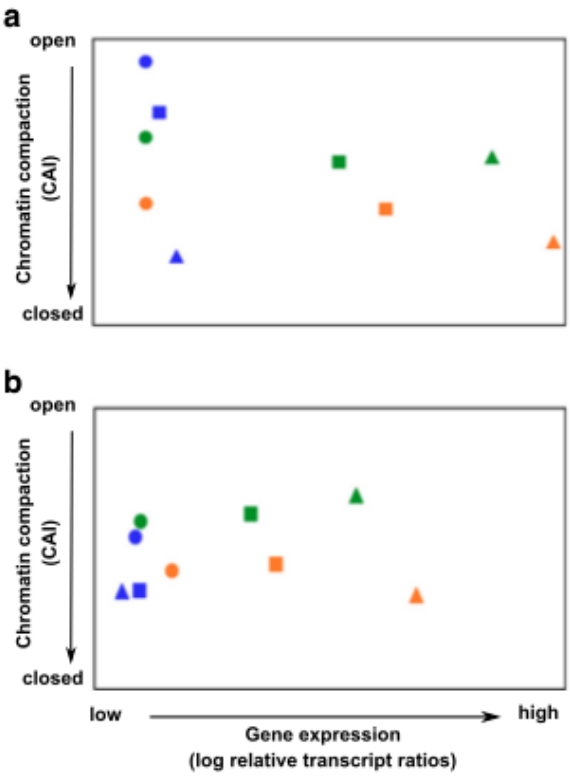

c

Gene	Spearman correlation	
	QM6a-CREI$_{96}$	QM6aΔ*cre1*
cbh1	-0.43 (*P*=0.5673)	0.31 (*P*=0.4473)
cbh2	-0.41 (*P*=0.2420)	-0.49 (*P*=0.0691)
xyr1	-0.84 (*P*=0.0375)	0.10 (*P*=0.7278)

Figure 6 Transcript and CHART analysis of *Trichoderma reesei* CREI-mutant strains during sophorose induction. QM6a-CREI$_{96}$ **(a)** and the Δ*cre1*-strain **(b)** were pre-grown on glycerol and thereafter incubated on sophorose for 30 (dots), 90 (boxes), and 180 (triangles) minutes. The *cbh1* (green), *cbh2* (orange), and *xyr1* (blue) genes were investigated. The gene expression analysis was performed by cDNA synthesis followed by qPCR, and transcript levels are depicted on the x-axis. CHART-PCR was performed by Dnase I digestion followed by qPCR, and CAIs are depicted on the y-axis. In both cases *sar1* and *act* genes were used for data normalization and QM6a-CREI$_{96}$ incubated for 30 minutes was the reference condition. All values are means from measurements in triplicates and three biological experiments (cultivations). Standard deviations were below 5%. Diagrams are identically scaled. **(c)** Spearman's rank correlation coefficients were calculated (close to −1 indicates negative correlation; close to 0 indicates no linear correlation; close to 1 indicates positive correlation). The *P*-values for each correlation coefficient were calculated to determine significance of data (how different from zero). $P > 0.05$ was considered as indicative of no linear correlation.

binding sites (compare Figures 2 and 3). Obviously, contacting of CREI-binding sites in target genes by CREI-96 leads to a more open chromatin in the core promoter regions under repressing conditions (D-glucose). As expected, this effect was not observed in such a pronounced manner under inducing conditions (sophorose), as the core promoter there already has an open chromatin. If CREI-96 develops this de-regulating function by simply binding the DNA (possibly in high amounts) and thereby preventing nucleosome assembly, or if it is involved in a more complicated chromatin-DNA interaction mechanism, cannot yet be answered and this calls for further investigation.

Secondly, CREI-96 acts on the chromatin structure in an indirect way. The transcript levels of the *htf1* gene encoding a chromatin-remodelling protein are upregulated in the presence of CREI-96. Notably, in the wild-type strain QM6a bearing the native CREI we found *htf1* downregulated, specifically on D-glucose (data not shown). This is in good accordance with previous studies, in which this gene was reported to be repressed by CREI in the *T. reesei* strain QM9414 [26] and to be lowly expressed in QM6a on D-glucose [31]. It can be speculated that CREI-96 in this case reverses the antagonistic function of CREI on chromatin-remodelling proteins and even supports the opening of chromatin in an indirect way.

Thirdly, the loss of the auto-regulatory function of CREI is very likely. It should be considered that surprisingly high transcript levels of *cre1-96* were detected in Rut-C30 (Figure 3a). In *A. nidulans* it was observed that a low steady-state level of *creA* mRNA can be increased within minutes by adding a repressing carbon source. While a prolonged incubation with the repressing carbon sources then led to auto-repression, the incubation on a de-repressing carbon source maintained the high level [18]. In Rut-C30 the *cre1-96* transcript levels on D-glucose are as high as on sophorose, indicating a loss of the mentioned native auto-repression. This might also be the reason for the generally higher abundance of transcript in Rut-C30 compared to the wild-type strain QM6a which we observed during this study. An alternative or additional explanation for the generally higher abundance of *cre1-96* in Rut-C30 is mRNA stability. This may arise from less stability of the mRNA coding for the full-length protein, or a general increase in mRNA stability speculated to be caused by two mutations (protein ID 110423 and 66895) identified in the direct ancestor of Rut-C30 (NG14) [11]. However, it can be assumed that in Rut-C30 this results in high amounts of CREI-96 present in the cell, which is still able to bind DNA, thereby possibly changing the chromatin status in CREI-target genes.

Even if in previous studies truncated forms of CREI have been investigated, interestingly, none of them reported a positive effect of the shorter CREI version compared to a deletion of CREI. This is most likely due to a different experimental design applied. Nakari-Setälä *et al.* reported similar cellulase activities (volumetrically given) of strains bearing a deletion or a truncation of CREI when grown on lactose [32]. However, the investigated strains exhibited different growth behaviors (biomass formation and CO_2-

Table 1 Investigated candidate genes encoding ATP-dependent chromatin remodelling factors

Protein ID	Annotation[a]	Provisory name
44747	Helicase-like transcription factor HLTF/DNA helicase RAD5, DEAD-box superfamily	*htf1 (snf2)*
57935	Chromatin remodelling complex SWI/SNF, component SWI2 and related ATPases (DNA/RNA helicase superfamily)/ATPase	*snf2-like*
21557	Chromatin remodelling factor subunit and related transcription factors	*rsc8*
57608	Chromatin remodelling complex WSTF-ISWI, small subunit	*isw1*
109526	Chromatin remodelling complex WSTF-ISWI, small subunit	*isw2*
50539	SNF2 family DNA-dependent ATPase	*ino80*
58928	Chromodomain-helicase DNA-binding protein	*cdh1*

[a]according to TRIRE Joint Genome Institute - JGI - *Trichoderma reesei* v2.0 database.

levels) [32]. In order to exclude any growth effects we studied a resting cell system under inducing conditions (sophorose). Such a highly standardized transfer experiment allows determination of the mechanistic influence of an isolated phenomenon (presence of CREI-96 or lack of CREI).

We also investigated growth conditions on D-glucose as this is certainly industrially relevant (enzyme production on high glucose-containing inducers). In this case we also observed differences in transcript levels between the two CREI mutant strains, which is in accordance with the results of a Northern analysis of *cbh1* on glucose by Nakari-Setälä *et al.* [32] and of the *cbh1* transcript level analysis by Ries *et al.* [24].

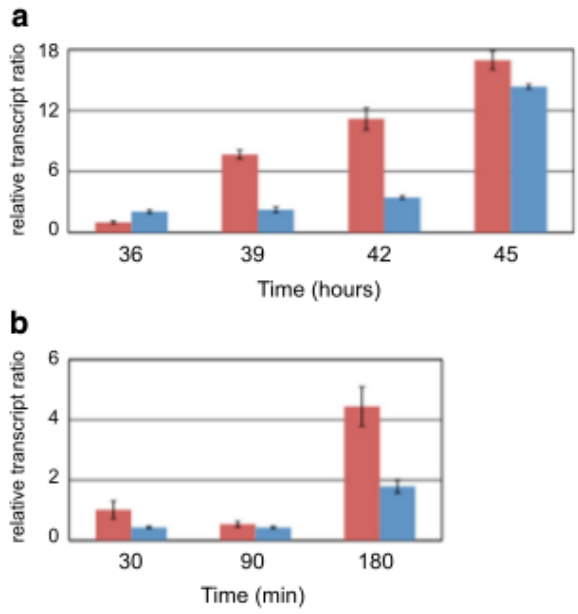

Figure 7 Transcript analysis of *htf1* in *Trichoderma reesei* CREI-mutant strains. QM6a-CREI$_{96}$ (red bars) and the Δ*cre1*-strain (blue bars) were grown on D-glucose and samples were drawn after 36, 39, 42, and 45 hours **(a)** or pre-grown on glycerol and transferred to sophorose for 30, 90, and 180 minutes **(b)**. The transcript levels were analyzed by qPCR using *sar1* and *act* genes for data normalization and levels refer to QM6a-CREI$_{96}$ grown for 36 hours or incubated for 30 minutes, respectively. The values are means from measurements in triplicates and three biological experiments (cultivations). Error bars indicate standard deviations.

We noticed that the increased transcript levels in strain QM6a-CREI$_{96}$ corresponded with an opening of chromatin on D-glucose, which was not found on sophorose. We propose that this different observation is likely due to the fact that the remodelling of chromatin usually becomes necessary under repressing conditions, while under inducing conditions certain regulatory factors and/or mechanisms have already ensured the open chromatin status. Obviously, the differences between the two CREI mutant strains observed on sophorose are primarily related to induction, chromatin opening, and expression of XYRI. During early-stage induction (30 minutes) the presence of sophorose leads to a rapid and higher chromatin accessibility of *xyr1* in QM6a-CREI$_{96}$, which subsequently results in higher *xyr1* transcript levels (Figure 6). It was previously reported that the level of *xyr1* expression is directly linked to the expression of *cbh1* and *cbh2* [6]. Accordingly, we detected higher *cbh1* and *cbh2* transcript levels in the QM6a-CREI$_{96}$ on sophorose.

Conclusions

From the result obtained during this study we conclude that the truncated version of CREI present in Rut-C30 (CREI-96) should be considered as a discrete transcription factor with different properties than CREI. It acts in a direct manner on target URRs, but also contributes indirectly to a more open chromatin status by regulating a chromatin remodeler. Altogether it should be considered that Rut-C30 not only lacks CREI and the thereby mediated CCR, but also gains the now positively acting regulatory protein CREI-96.

Orthologs of CREI regulate CCR in numerous filamentous fungi including those used in biofuel production. Unfortunately, a simple deletion of *cre1* does not only lead to the desired release from CCR, but also to severe growth impairment. Consequently, molecular strain design can alternatively be based on the described CREI-96 truncation. This strategy does on one hand avoid growth

deficiencies and the accompanying loss of productivity, and on the other hand additionally leads to a chromatin remodelling effect that results in increased expression of PCW-degrading enzymes.

Materials and Methods

Fungal strains

The following *T. reesei* strains were used throughout this study: the wild-type strain QM6a (ATCC 13631), Rut-C30, which was described as a high yielding cellulase mutant of QM6a (ATCC 56765) [10], a *cre1* deletion in QM6a (Δ*cre1*) [32], a 83 kb deletion corresponding to the large deletion in scaffold 15 of Rut-C30 in QM6aΔ*tmus53* (Δscaff15) [13,33], as well as a QM6aΔ*tmus53* strain bearing the truncated *cre1* of Rut-C30 (QM6a-CREI$_{96}$) constructed during this study. All strains were maintained on malt extract agar or potato-dextrose-agar.

Growth conditions

For carbon source replacement experiments mycelia were pre-cultured in 1 L Erlenmeyer flasks on a rotary shaker (180 rpm) at 30°C for 24 hours in 250 mL of Mandels-Andreotti (MA) medium [34] supplemented with 1% (w/v) glycerol as sole carbon source. A total of 10^9 conidia per litre (final concentration) were used as inoculum. Pre-grown mycelia were washed and equal amounts were resuspended in 20 ml MA media containing 1% (w/v) D-glucose or 2 mM sophorose (Serva Electrophoresis, Heidelberg, Germany) as sole carbon source, or no carbon source respectively, and incubated for 30 minutes to 3 hours. For direct cultivation experiments the conidia were incubated in 250 mL Erlenmeyer flasks on a rotary shaker (180 rpm) at 30°C for 45 hours in 50 mL of MA medium supplemented with 1% (w/v) D-glucose as sole carbon source. Samples were derived from three biological replicates and were pooled before RNA extraction and chromatin digestion.

Replacement of CREI in *T. reesei* QM6a

Transformation of *T. reesei* QM6aΔ*tmus53* [33] was performed using two overlapping 3 kb-DNA fragments. The first fragment consisted of the truncated *cre1* of Rut-C30 amplified with primers RG186 and RG187 using genomic DNA as template and 3′-half of the expression cassette bearing the *Escherichia coli hph* marker gene amplified with primers RG188 and hph3′_fw using the plasmid pRLMex$_{30}$ [35] as template. The second fragment consisted of the 5′-half of the expression cassette bearing the *E. coli hph* marker gene amplified with primers hph5′_rev and RG189 using pRLMex$_{30}$ as template and the *cre1* 3′-flank from Rut-C30 amplified with primers RG190 and RG191 using genomic DNA as template. Protoplast transformation of QM6a was performed as described in United States patent number 8,323,931 using 2.5 μg of each DNA fragment in a co-transformation. Genomic integration of the full construct (*cre1-96*::*hph*) into the *cre1* locus was confirmed by southern blot analysis and DNA sequencing (Microsynth, Balgach, Switzerland).

In vivo footprinting

In vivo methylation using DMS followed by ligation-mediated PCR was performed as described previously [27]. FAM (fluorescein amidite)-labelled fragments were analyzed by capillary gel electrophoresis (Microsynth) and results were analyzed using ivFAST [27].

Analysis of transcript levels

Fungal mycelia were homogenized in 1 mL of peqGOLD-TriFast DNA/RNA/protein purification system reagent (PEQLAB Biotechnologie, Erlangen, Germany) using a FastPrep(R)-24 cell disrupter (MP Biomedicals, Santa Ana, California, United States). RNA was isolated according to the manufacturer's instructions, and the concentration was measured using the NanoDrop 1000 (Thermo Scientific, Waltham, Massachusetts, United States). Synthesis of cDNA from mRNA was carried out using the RevertAidTM H Minus First Strand cDNA Synthesis Kit (Thermo Scientific, Waltham, Massachusetts, United States) according to the manufacturer's instructions. Quantitative PCRs were performed in a Rotor-Gene Q system (Qiagen, Hilden, Germany). All reactions were performed in triplicate. The amplification mixture (final volume 15 μL) contained 7.5 μL 2 × iQ SYBR Green Mix (Bio-Rad, Hercules, USA), 100 nM forward and reverse primer, and 2.5 μL cDNA (diluted 1:20). Primer sequences are provided in Table 2. Cycling conditions and control reactions were performed as described previously [36]. Data normalization using *sar1* and *act* as reference genes and calculations were performed as published previously [36].

Plasmid construction

A 307 bp fragment was amplified from Rut-C30 genomic DNA using primers RG182 and RG178 and was inserted into the expression vector pGEX-4 T-2 (GE Healthcare Life Sciences, Little Chalfont, Buckinghamshire, United Kingdom) via *BamH*I/*Xho*I digestion yielding the plasmid pGEX-cre1-RG182 for heterologous expression of GST (glutathione S-transferase)-fused CREI-96.

Protein expression and purification

E. coli BL21(DE3)pLysS (Promega, Madison, Wisconsin, United States) carrying pGEX-cre1-RG182 was cultivated in a 1 L Erlenmeyer flask on a rotary shaker (200 rpm) at 37°C in 300 mL LB medium supplemented with ampicillin (50 μg/mL) until an OD_{600} of 0.5 was reached. Protein expression was induced by adding IPTG to a final concentration of 0.5 mM followed by an incubation at 37°C for 3 hours. The cells were harvested by centrifugation and

Table 2 Oligonucleotides used in this study

Name	Sequence (5' - 3')	Usage
RG53	GAATTCAGATC	iv-FP, oligo-short
RG54	GCGGTGACCCGGGAGATCTGAATTC	iv-FP, oligo-long
RG89	[6-FAM]GTAGAGGCATGTTGTGAATCTGTGTCGGG	iv-FP, cbh1oligo3fw, EMSA
RG90	[6-FAM]GGTTGTATGCAAAACGCTCCGAGTCAGAC	iv-FP, cbh1oligo3rev, EMSA
RG215	CCAACGGCTT*GTGGGG*TTGCAGAAGCAACGGCAAAGCCCC*ACTTCCCCAC*GTTTGTTTCT[a]	EMSA
RG216	AGAAACAAAC*GTGGGGAAGTGGGG*CTTTGCCGTTGCTTCTGCAA*CCCCACAAGCC*GTTGG	
RG221	CCAACGGCTTGTT**T**GGGTTGCAGAAGCAACGGCAAAGCCC**A**ACTTCCC**A**ACGTTTGTTTCT[b]	
RG222	AGAAACAAAC*GTT**T**GGGAAGTT**T**GGG*CTTTGCCGTTGCTTCTGCAA*CCC**A**ACAAGCC*GTTGG	
RG178	TATCTCGAGTTTAGAAAAAAAAGCAGGT	pGEX-cre1-RG182 construction
RG182	ATTGGATCCATGCAACGAGCACAGTCTGCCGT	
RG186	TTGAGTGCAGACGTGTGTGTAATCTT	Construction of QM6a-CREI$_{96}$
RG187	CCCTCCTTTGTTAGAAAAAAAAGCAGGTAATGG	
RG188	TTTTTTCTAACAAAGGAGGGAGACGAGGTTG	
RG189	CCTACATTGGATAACGGTGAGACTAGCGGCC	
RG190	TCACCGTTATCCAATGTAGGTAAGTAGTAAGGG	
RG191	GAATCAGTATTTTCTCATCTCCTTG	
hph3'_fw	GACCTGCCTGAAACCGAACTG	
hph5'_rev	GAAGAAGATGTTGGCGACCTCG	
actfw	TGAGAGCGGTGGTATCCACG	qPCR
actrev	GGTACCACCAGACATGACAATGTTG	
sar1fw	TGGATCGTCAACTGGTTCTACGA	
sar1rev	GCATGTGTAGCAACGTGGTCTTT	
cbh1f	GATGATGACTACGCCAACATGCTG	
cbh1r	ACGGCACCGGGTGTGG	
cbh2f	CTATGCCGGACAGTTTGTGGTG	
cbh2r	GTCAGGCTCAATAACCAGGAGG	
xyr1f	CCCATTCGGCGGAGGATCAG	
xyr1r	CGAATTCTATACAATGGGCACATGGG	
44747f	GCTCGAGCTGCAAGACAAGA	
44747r	GCGGAGATCCATGAGCTTCT	
epiactinTr_f	CTTCCCTCCTTTCCTCCCCCTCCAC	act CHART, region −226 to +24
epiactinTr_r	GCGACAGGTGCACGTACCCTCCATT	
episar1Tr_f	GTCAGGAAATGCCGCACAAGCAAGA	sar1 CHART, region −490 to −224
episar1Tr_r	TGTGTTTTACCGCCTTGGCCTTTGG	
epicbh1_2Tr_f	GGATCGAACACACTGCTGCCTTTAC	cbh1 CHART, region −301 to −27
epicbh1_2Tr_r	GGTTTCTGTGCCTCAAAAGATGGTG	
epicbh2_2Tr_f	TGCAGCGCAACACTACACGCAACAT	cbh2 CHART, region −355 to −62
epicbh2_2Tr_r	TGCGCCTCATACAGGGTCACAGTCC	
epixyr1_2Tr_f	CCGACAGCAGCAGTAGTCAGGTTTT	xyr1 CHART, region −216 to +35
epixyr1_2Tr_r	TAGGCAGAATAGCGACGGAGAGGAT	

[a]Italic letters indicate a CREI-binding site (5'-SYGGRG-3').
[b]Bold letters indicate the introduced mutation in the CREI-binding site (5'-SYTGRG-3').

stored at −20°C overnight. GST-fusion protein (theoretical molecular weight 37 kDa) was purified from *E. coli* cell lysates using Glutathione-Superflow Resin (Qiagen, Hilden, Germany) according to the manufacturer's instructions.

Electrophoretic mobility shift assay (EMSA)

A 400-bp PCR product comprising the part of the 5′-URR region of *cbh1*, which contains 3 CREI-binding sites, was obtained with FAM-labelled primers RG89 and RG90 and used as probe (Table 2). The protein-DNA binding assay and non-denaturing polyacrylamide gel electrophoresis were performed essentially as previously described [37]. Binding was achieved by incubating increasing amounts of heterologously expressed, thrombin-cleaved CREI-96 (500 nM, 1000 nM, and 2000 nM) with 4 ng of the labelled, double-stranded DNA fragment in GST elution buffer (10 minutes at 22°C). Fluorescence and image analysis of the gels was carried out using a Typhoon 8600 variable mode imager (Amersham Bioscience, part of GE Healthcare, Little Chalfont, Buckinghamshire, United Kingdom). Competition experiments were performed using 2000 nM of protein together with increasing amounts (50-fold, 100-fold, and 200-fold) of either a cold competitor (an unlabeled double-stranded DNA probe obtained by annealing primers RG215 and RG216) or a mutated cold competitor (an unlabeled double-stranded DNA probe obtained by annealing primers RG221 and RG222). This probe bears in all three CREI-binding sites a mutation from 5′-SYGGRG-3′ to 5′-SYTGRG-3′, which was previously shown to prevent the binding of CREI *in vivo* and *in vitro* [21].

Determination of cellulase activity

Cellulase activity in the culture supernatants was determined using AZCL HE-Cellulose (Megazyme International, Bray, Ireland) in 25 mM sodium acetate buffer pH 4.5 according to the manufacturer's instructions. To measure biomass (dry weight), the cultures were harvested by filtration, washed with an equal volume of 0.8% NaCl solution, dried at 80°C for 24 hours, and weighed. Samples from two biological replicates and two technical replicates were measured.

Chromatin accessibility real-time PCR (CHART-PCR)

DNase I digestion of chromatin and DNA extraction were carried out as described by Gonzalez and Scazzocchio [38] with minor modifications. Mycelia were harvested by filtration, pressed dry with filter paper, frozen in liquid nitrogen, and ground to a fine powder. Portions (100 mg) of the powder were suspended in 1 mL aliquots of nuclease digestion buffer (250 mM sucrose, 60 mM KCl, 15 mM NaCl, 0.05 mM $CaCl_2$, 3 mM $MgCl_2$, 0.5 mM DTT, and 15 mM Tris-HCl at pH 7.5), and 100-μL samples of the digestion mixture were incubated with 10 U of RQ1 RNase-free DNase I (Promega, Madison, Wisconsin, United States) for 2.5 minutes at 37°C. The reaction was stopped by adding 100 μL of 40 mM EDTA and 2% SDS, followed by two rounds of phenol-chloroform extraction and one round of chloroform extraction. Samples were then treated with 10 μg/mL of RNase A for 15 minutes at 37°C and precipitated with ethanol. DNA pellets were suspended in 100 μL of 5 mM Tris-HCl at pH 7.5. A control without DNase I was included to monitor endonuclease activity. qPCR analysis of the DNase I-treated samples was performed to measure the relative abundance of target regions. PCRs were performed in a Rotor-Gene Q system (Qiagen, Hilden, Germany). All reactions were performed in triplicate. The amplification mixture (final volume 20 μL) contained 10 μL 2 × iQ SYBR Green Mix (Bio-Rad, Hercules, USA), 200 nM forward and reverse primers and 10 ng of DNA. Primer sequences are provided in Table 2. Cycling conditions were as follows: 3 minutes initial denaturation at 95°C, followed by 40 cycles of 15 seconds at 95°C and 60 seconds at 60°C. The amount of intact input DNA of each sample was calculated by comparing the threshold values of the PCR amplification plots with a standard curve generated for each primer set using serial dilutions of genomic, undigested DNA. The chromatin accessibility index (CAI) was defined as:

$$\mathrm{CAI} = 1/(\mathrm{Ds}/((\mathrm{Dc1} + \mathrm{Dc2})/2)) \quad (1)$$

where Ds is the amount of intact DNA detected for each target region and Dc1 and Dc2 are the amounts of intact DNA detect for the promoter regions of *sar1* and *act* respectively, used as reference genes for normalization.

To access the relationship between the CAI and the transcript level, a two-tailed Spearman's rank correlation coefficient was determined for each gene analyzed. The *P*-value for each correlation coefficient was calculated to determine the significance of the data.

Selection of investigated genes encoding chromatin remodelling factors

Genes were selected by direct searching for SNF2, ISW1, ISW2, INO80, CDH1, RSC8 (the most prominent chromatin remodelling-related proteins characterized in yeast) in the *T. reesei* genome database [39]. Additional candidate genes were obtained by using BLASTp (basic local alignment search tool) search in the NCBI database employing respective *S. cerevisiae* sequences as baits to identify similar sequences in filamentous fungi. Subsequently, these sequences were used in a BLAST search in the *T. reesei* database.

Abbreviations

BLAST: Basic local alignment search tool; CAI: Chromatin accessibility index; CHART-PCR: Chromatin accessibility real-time PCR; CREI: Carbon catabolite repressor 1; DMS: Dimethyl sulphate; EMSA: Electrophoretic mobility shift assay; GST: Glutathione S-transferase; ivFAST: *in vivo* footprinting analysis

software tool; MA: Mandels-Andreotti; PCW: Plant cell wall; RT-qPCR: Reverse transcription quantitative PCR; URR: Upstream regulatory region; XYR1: Xylanase regulator 1.

Competing interests
The authors declare that they have no competing interests.

Authors' contributions
RG constructed the strain bearing the truncated version of CREL TMMS carried out transcript analyses, CHART-PCR, and EMSA. AR carried out the *in vivo* footprinting analyses. MJPF participated in conception of the study and revised the manuscript critically. RLM participated in conception of the study. ARMA participated in conception of the study, supervised the experiments, and prepared the manuscript. All authors read and approved the final manuscript.

Acknowledgements
This study was supported by two grants from the Austrian Science Fund (FWF; grant numbers V232-B20 and P24851) given to ARM-A. The recombinant QM6a strains Δ*cre1* and Δscaff15 used in this study were originally created at VTT Technical Research Centre of Finland and their receipt is gratefully acknowledged. We thank René Mayer for his help in performing appropriate statistical tests.

Author details
[1]Department for Biotechnology and Microbiology, Institute of Chemical Engineering, Vienna University of Technology, Gumpendorfer Str. 1a, A-1060 Wien, Austria. [2]Department of Genetics and Morphology, Institute of Biological Sciences, University of Brasília, Campus Universitário Darcy Ribeiro, 70910-900 Brasília, DF, Brazil.

Received: 5 June 2014 Accepted: 22 August 2014
Published online: 11 September 2014

References
1. Martinez D, Berka RM, Henrissat B, Saloheimo M, Arvas M, Baker SE, Chapman J, Chertkov O, Coutinho PM, Cullen D, Danchin EG, Grigoriev IV, Harris P, Jackson M, Kubicek CP, Han CS, Ho I, Larrondo LF, de Leon AL, Magnuson JK, Merino S, Misra M, Nelson B, Putnam N, Robbertse B, Salamov AA, Schmoll M, Terry A, Thayer N, Westerholm-Parvinen A, *et al*: **Genome sequencing and analysis of the biomass-degrading fungus *Trichoderma reesei* (syn. *Hypocrea jecorina*).** *Nat Biotechnol* 2008, **26**:553–560.
2. Teeri T, Salovouri I, Knowles J: **The molecular cloning of the major cellulase gene from *Trichoderma reesei*.** *Biotechnology* 1983, **1**:696–699.
3. Buchert J, Oksanen T, Pere J, Siika-aho M, Suurnäkki A, Viikari L: **Applications of *Trichoderma reesei* Enzymes in the Pulp and Paper Industry.** In *Trichoderma & Gliocladium*, Volume 2. Edited by Kubicek CP, Harman GE. London: Taylor & Francis; 1998:343–357.
4. Galante YM, de Conti A, Monteverdi R: **Application of *Trichoderma* Enzymes in the Food and Feed Industries.** In *Trichoderma & Gliocladium*, Volume 2. Edited by Kubicek CP, Harman GE. London: Taylor & Francis; 1998:327–342.
5. Galante YM, de Conti A, Monteverdi R: **Application of *Trichoderma* Enzymes in the Textile Industry.** In *Trichoderma & Gliocladium*, Volume 2. Edited by Kubicek CP, Harman GE. London: Taylor & Francis; 1998:311–325.
6. Derntl C, Gudynaite-Savitch L, Calixte S, White T, Mach RL, Mach-Aigner AR: **Mutation of the Xylanase regulator 1 causes a glucose blind hydrolase expressing phenotype in industrially used *Trichoderma* strains.** *Biotechnol Biofuels* 2013, **6**:62.
7. Peterson R, Nevalainen H: ***Trichoderma reesei* RUT-C30 - thirty years of strain improvement.** *Microbiology* 2012, **158**:58–68.
8. Montenecourt BS, Eveleigh DE: **Semiquantitative plate assay for determination of cellulase production by *Trichoderma viride*.** *Appl Environ Microbiol* 1977, **33**:178–183.
9. Montenecourt BS, Eveleigh DE: **Preparation of mutants of *Trichoderma reesei* with enhanced cellulase production.** *Appl Environ Microbiol* 1977, **34**:777–782.
10. Montenecourt BS, Eveleigh DE: **Selective Screening Methods for the Isolation of High Yielding Cellulase Mutants of *Trichoderma reesei*.** In *Hydrolysis of Cellulose: Mechanisms of Enzymatic and Acid Catalysis*, Volume 181. Edited by Brown RD, Jurasek L. Washington DC: American Chemical Society; 1979:289–301.
11. Le Crom S, Schackwitz W, Pennacchio L, Magnuson JK, Culley DE, Collett JR, Martin J, Druzhinina IS, Mathis H, Monot F, Seiboth B, Cherry B, Rey M, Berka R, Kubicek CP, Baker SE, Margeot A: **Tracking the roots of cellulase hyperproduction by the fungus *Trichoderma reesei* using massively parallel DNA sequencing.** *Proc Natl Acad Sci U S A* 2009, **106**:16151–16156.
12. Seidl V, Gamauf C, Druzhinina IS, Seiboth B, Hartl L, Kubicek CP: **The *Hypocrea jecorina* (*Trichoderma reesei*) hypercellulolytic mutant RUT C30 lacks a 85 kb (29 gene-encoding) region of the wild-type genome.** *BMC Genomics* 2008, **9**:327.
13. Vitikainen M, Arvas M, Pakula T, Oja M, Penttilä M, Saloheimo M: **Array comparative genomic hybridization analysis of *Trichoderma reesei* strains with enhanced cellulase production properties.** *BMC Genomics* 2010, **11**:441.
14. Strauss J, Mach RL, Zeilinger S, Hartler G, Stoffler G, Wolschek M, Kubicek CP: **Cre1, the carbon catabolite repressor protein from *Trichoderma reesei*.** *FEBS Lett* 1995, **376**:103–107.
15. Ilmén M, Thrane C, Penttilä M: **The glucose repressor gene *cre1* of *Trichoderma*: isolation and expression of a full-length and a truncated mutant form.** *Mol Gen Genet* 1996, **251**:451–460.
16. Bailey C, Arst HN Jr: **Carbon catabolite repression in *Aspergillus nidulans*.** *Eur J Biochem* 1975, **51**:573–577.
17. Drysdale MR, Kolze SE, Kelly JM: **The *Aspergillus niger* carbon catabolite repressor encoding gene, *creA*.** *Gene* 1993, **130**:241–245.
18. Strauss J, Horvath HK, Abdallah BM, Kindermann J, Mach RL, Kubicek CP: **The function of CreA, the carbon catabolite repressor of *Aspergillus nidulans*, is regulated at the transcriptional and post-transcriptional level.** *Mol Microbiol* 1999, **32**:169–178.
19. Nehlin JO, Carlberg M, Ronne H: **Control of yeast GAL genes by MIG1 repressor: a transcriptional cascade in the glucose response.** *EMBO J* 1991, **10**:3373–3377.
20. Ilmén M, Onnela ML, Klemsdal S, Keranen S, Penttilä M: **Functional analysis of the cellobiohydrolase I promoter of the filamentous fungus *Trichoderma reesei*.** *Mol Gen Genet* 1998, **257**:386.
21. Mach RL, Strauss J, Zeilinger S, Schindler M, Kubicek CP: **Carbon catabolite repression of xylanase I (*xyn1*) gene expression in *Trichoderma reesei*.** *Mol Microbiol* 1996, **21**:1273–1281.
22. Mach-Aigner AR, Pucher ME, Steiger MG, Bauer GE, Preis SJ, Mach RL: **Transcriptional regulation of *xyr1*, encoding the main regulator of the xylanolytic and cellulolytic enzyme system in *Hypocrea jecorina*.** *Appl Environ Microbiol* 2008, **74**:6554–6562.
23. Stricker AR, Grosstessner-Hain K, Würleitner E, Mach RL: **Xyr1 (xylanase regulator 1) regulates both the hydrolytic enzyme system and D-xylose metabolism in *Hypocrea jecorina*.** *Eukaryot Cell* 2006, **5**:2128–2137.
24. Ries L, Belshaw NJ, Ilmén M, Penttilä ME, Alapuranen M, Archer DB: **The role of CRE1 in nucleosome positioning within the *cbh1* promoter and coding regions of *Trichoderma reesei*.** *Appl Microbiol Biotechnol* 2014, **98**:749–762.
25. Zeilinger S, Schmoll M, Pail M, Mach RL, Kubicek CP: **Nucleosome transactions on the *Hypocrea jecorina* (*Trichoderma reesei*) cellulase promoter *cbh2* associated with cellulase induction.** *Mol Genet Genomics* 2003, **270**:46–55.
26. Portnoy T, Margeot A, Linke R, Atanasova L, Fekete E, Sandor E, Hartl L, Karaffa L, Druzhinina IS, Seiboth B, Le Crom S, Kubicek CP: **The CRE1 carbon catabolite repressor of the fungus *Trichoderma reesei*: a master regulator of carbon assimilation.** *BMC Genomics* 2011, **12**:269.
27. Gorsche R, Jovanovic B, Gudynaite-Savitch L, Mach RL, Mach-Aigner AR: **A highly sensitive *in vivo* footprinting technique for condition-dependent identification of *cis* elements.** *Nucleic Acids Res* 2014, **42**:e1.
28. Cziferszky A, Mach RL, Kubicek CP: **Phosphorylation positively regulates DNA binding of the carbon catabolite repressor Cre1 of *Hypocrea jecorina* (*Trichoderma reesei*).** *J Biol Chem* 2002, **277**:14688–14694.
29. Manfield IW, Reynolds LA, Gittins J, Kneale GG: **The DNA-binding domain of the gene regulatory protein AreA extends beyond the minimal zinc-finger region conserved between GATA proteins.** *Biochim Biophys Acta* 2000, **1493**:325–332.
30. Abrams E, Neigeborn L, Carlson M: **Molecular analysis of SNF2 and SNF5, genes required for expression of glucose-repressible genes in *Saccharomyces cerevisiae*.** *Mol Cell Biol* 1986, **6**:3643–3651.
31. Ries L, Pullan ST, Delmas S, Malla S, Blythe MJ, Archer DB: **Genome-wide transcriptional response of *Trichoderma reesei* to lignocellulose using RNA sequencing and comparison with *Aspergillus niger*.** *BMC Genomics* 2013, **14**:541.
32. Nakari-Setälä T, Paloheimo M, Kallio J, Vehmaanperä J, Penttilä M, Saloheimo M: **Genetic modification of carbon catabolite repression in *Trichoderma***

reesei for improved protein production. *Appl Environ Microbiol* 2009, **75**:4853–4860.
33. Steiger MG, Vitikainen M, Uskonen P, Brunner K, Adam G, Pakula T, Penttilä M, Saloheimo M, Mach RL, Mach-Aigner AR: **Transformation system for *Hypocrea jecorina* (*Trichoderma reesei*) that favors homologous integration and employs reusable bidirectionally selectable markers.** *Appl Environ Microbiol* 2011, **77**:114–121.
34. Mandels M: **Applications of cellulases.** *Biochem Soc Trans* 1985, **13**:414–416.
35. Mach RL, Schindler M, Kubicek CP: **Transformation of *Trichoderma reesei* based on hygromycin B resistance using homologous expression signals.** *Curr Genet* 1994, **25**:567–570.
36. Steiger MG, Mach RL, Mach-Aigner AR: **An accurate normalization strategy for RT-qPCR in *Hypocrea jecorina* (*Trichoderma reesei*).** *J Biotechnol* 2010, **145**:30–37.
37. Stangl H, Gruber F, Kubicek CP: **Characterization of the *Trichoderma reesei cbh2* promoter.** *Curr Genet* 1993, **23**:115–122.
38. Gonzalez R, Scazzocchio C: **A rapid method for chromatin structure analysis in the filamentous fungus *Aspergillus nidulans*.** *Nucleic Acids Res* 1997, **25**:3955–3956.
39. **Joint Genome Institute *Trichoderma reesei* v2.0.** http://genome.jgi-psf.org/Trire2/Trire2.home.html.

doi:10.1186/s13068-014-0129-3
Cite this article as: Mello-de-Sousa *et al.*: A truncated form of the Carbon catabolite repressor 1 increases cellulase production in *Trichoderma reesei*. *Biotechnology for Biofuels* 2014 **7**:129.

Acknowledgements

I would like to thank Robert Mach and Astrid Mach-Aigner for the supervision and the opportunity to do my doctoral thesis in their working group. I would like to thank especially my colleagues Thiago Mello de Sousa and Christian Derntl, who sacrificed a bit of their precious time to revise my thesis very critically. A big thank you to my other colleagues Daniel Kiesenhofer, Petra Till, Ina Regnat and Domenico Kitty Savio for their support, advices and the nice working atmosphere. And I won't forget the nice coffee breaks with Jonas Ramoni and Romi Gaderer.

Above all, I would like to thank my parents Bernhard and Andrea, my grandparents Ingrid and Walter and my sister Ines, not forgetting my dear friend Pubsi Pokorny. I wouldn't have made it this far without all of you.

Last but not least, I would like to thank Andreas Puna Schüller. Thank you for always being there for me and believing in me.

Curriculum Vitae

DI Alice Rassinger, BSc

Wallgasse 30/9-10
1060 Wien
alice.rassinger@tuwien.ac.at
+43 (1) 58801-166582

Persönliche Angaben

Geboren am 05.03.1988 in St. Pölten (Niederösterreich)
Staatsbürgerschaft: Österreich
Ledig

Ausbildung

Technische Universität Wien

08/2013 – 06/2017	Dissertation Effectors of DNA accessibility in *Trichoderma reesei*
10/2010 – 06/2013	Masterstudium Biotechnologie und Bioanalytik Chromatin rearrangement analysis of Xyr1 regulon genes in *Trichoderma reesei*
10/2006 – 10/2010	Bakkalaureatsstudium der Technischen Chemie

Bundesgymnasium und Bundesrealgymnasium, Piaristengasse 2, Krems

1998 – 2006	Abschluss mit Reifeprüfung

Auslandssemester

Chalmers University of Technology in Göteborg, Schweden

01/2012 – 05/2012	Auslandsaufenthalt mit einem Mobilitätsstipendium (Erasmus)

Berufserfahrung

Projekte der Abteilung für Genderkompetenz und Frauenförderung, TU Wien

07/2015	Tätigkeit als Unterstützerin von Organisation, experimenteller Gestaltung und Materialbeschaffung für den techNIKE Workshop „Tanz der Moleküle“ für 10-15 jährige Mädchen.
10/2012 – 10/2015	Online Mentorin für SchülerInnen ab 16 Jahren und StudienanfängerInnen der TU Wien.
07/2011 – 07/2014	Tätigkeit als Trainerin im Rahmen der techNIKE Workshops „Seife & Co“ und „Tanz der Moleküle“ für 10-15 jährige Mädchen.

Sprachkenntnisse & sonstige Qualifikationen

Sprachen

Deutsch: Muttersprache
Englisch: fließend in Wort und Schrift
Französisch: Grundkenntnisse in Wort und Schrift

Sonstige Qualifikationen

ECDL in MS Office

Wissenschaftliche Publikationen

Zeitschriftenartikel in „peer-reviewed" Journalen

Rassinger, A.*, Mello-de-Sousa, T. M.*, Regnat K., Derntl C., Mach, R. L., Mach-Aigner, A. R. (2016) The Relation Between Promoter Chromatin Status, Xyr1 and Cellulase Ex-pression in *Trichoderma reesei*. *Mycosphere* **8(3)** 432-444
* gleichwertige Erstautorenschaften

Derntl, C., **Rassinger, A.**, Srebotnik, E., Mach, R. L., Mach-Aigner, A. R. (2016) Identification of the Main Regulator Responsible for Synthesis of the Typical Yellow Pigment Produced by *Trichoderma reesei*. *Appl Environ Microbiol* **82(20)**:6247-6257. Print 2016 Oct 15.

Mello-de-Sousa, T. M.*, **Rassinger, A**.*, Derntl C., Poças Fonseca, M. J., Mach, R. L., Mach-Aigner, A. R. (2016) The Relation Between Promoter Chromatin Status, Xyr1 and Cellulase Ex-pression in *Trichoderma reesei*. *Curr Genomics* **17(2):**145-52. doi: 10.2174/1389202917666151116211812
* gleichwertige Erstautorenschaften

Mello-de-Sousa, T. M., **Rassinger, A.**, Pucher, M. E., dos Santos Castro, L., Persinoti, G.F., Silva-Rocha, R., Poças Fonseca, M. J., Mach, R. L., Nascimento Silva, R., Mach-Aigner, A. R. (2015) The impact of chromatin remodelling on cellulase expression in *Trichoderma reesei. BMC Genomics* **16**:588. doi: 10.1186/s12864-015-1807-7

Derntl, C., **Rassinger, A.**, Srebotnik, E., Mach, R. L., Mach-Aigner, A. R. (2015) Xpp1 regulates expression of xylanases but not of cellulases in *Trichoderma reesei. Biotechnol Biofuels* **8**:112. doi: 10.1186/s13068-015-0298-8

Mello-de-Sousa, T. M., Gorsche, R., **Rassinger, A.**, Poças Fonseca, M. J., Mach, R. L., Mach-Aigner, A. R. (2014) A truncated form of the Carbon catabolite repressor 1 increases cellulase production in *Trichoderma reesei*. *Biotechnol Biofuels* **7**:129 doi: 10.1186/s13068-014-0129-3

Postervorträge

29th Fungal Genetics Conference, Pacific Grove, CA, USA (2017)

,The truncated version of Cre1 (Cre1-96) in cellulase production in *Trichoderma reesei*'

13th European Conference on Fungal Genetics, Paris, Frankreich (2016)

,Impact of inducer molecules on DNA accessibility in cellulase and xylanase gene expression in *Trichoderma reesei*'

6th ÖGMBT Annual Meeting, Wien, Österreich (2014)

,Can a truncated version overcome the absence of a repressor in terms of enhanced cellulase production in *Trichoderma reesei* ?'